

Accepted Manuscript

Title: Re-Os geochronology of the Neoproterozoic – Cambrian Dalradian Supergroup of Scotland and Ireland: Implications for Neoproterozoic stratigraphy, glaciations and Re-Os systematics

Authors: Alan D. Rooney, David M. Chew, David Selby

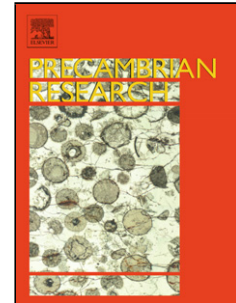
PII: S0301-9268(11)00011-8
DOI: doi:10.1016/j.precamres.2011.01.009
Reference: PRECAM 3337

To appear in: *Precambrian Research*

Received date: 13-7-2010
Revised date: 10-12-2010
Accepted date: 7-1-2011

Please cite this article as: Rooney, A.D., Chew, D.M., Selby, D., Re-Os geochronology of the Neoproterozoic – Cambrian Dalradian Supergroup of Scotland and Ireland: Implications for Neoproterozoic stratigraphy, glaciations and Re-Os systematics, *Precambrian Research* (2008), doi:10.1016/j.precamres.2011.01.009

This is a PDF file of an unedited manuscript that has been accepted for publication. As a service to our customers we are providing this early version of the manuscript. The manuscript will undergo copyediting, typesetting, and review of the resulting proof before it is published in its final form. Please note that during the production process errors may be discovered which could affect the content, and all legal disclaimers that apply to the journal pertain.



1 **Re-Os geochronology of the Neoproterozoic – Cambrian Dalradian**
2 **Supergroup of Scotland and Ireland: Implications for Neoproterozoic**
3 **stratigraphy, glaciations and Re-Os systematics**

4

5 Alan D. Rooney^{1*}, David M. Chew², David Selby¹

6 ¹Department of Earth Sciences, University of Durham, DH1 3LE, UK

7 ²Department of Geology, Trinity College Dublin, Dublin 2, Ireland

8 * Corresponding author: Tel. +44 0191 334 2300; Fax. +44 0191 334 2301.

9 *E-mail address:* alan.rooney@durham.ac.uk (A.D. Rooney).

10

11 **Abstract**

12 New Re-Os geochronology for the Ballachulish Slate Formation of the Dalradian
13 Supergroup, Scotland yields a depositional age of 659.6 ± 9.6 Ma. This age represents the
14 first successful application of the Re-Os system to rocks that have extremely low Re and
15 Os abundances (<1 ppb and <50 ppt, respectively). The Re-Os age represents a maximum
16 age for the glaciogenic Port Askaig Formation and refutes previous chemostratigraphic
17 and lithostratigraphic studies which correlated the Port Askaig Formation with a series of
18 middle Cryogenian (ca. 715 Ma) glacials. Additionally, the Re-Os age strongly suggests
19 that the Port Askaig Formation may be correlative with the ~ 650 Ma end-Sturtian
20 glaciations of Australia. As a consequence, the correlation of the Ballachulish Limestone
21 Formation with the ca. 800 Ma Bitter Springs anomaly is not tenable. Initial Os isotope
22 data from the Ballachulish Slate Formation coupled with data from Australia reveals a
23 radiogenic $^{187}\text{Os}/^{188}\text{Os}$ isotope composition (~ 0.8 to 1.0) for seawater during the
24 Neoproterozoic, which is similar to that of modern seawater (1.06).

25 We also report a young, highly imprecise Re-Os age (310 ± 110 Ma) for the Early
26 Cambrian Leny Limestone Formation which is constrained biostratigraphically by a
27 polymerid and miomerid trilobite fauna. We suggest, based on the mineralogy of the
28 Leny Limestone, (kaolinite, muscovite and a serpentine group mineral, berthierine), that
29 the Re-Os systematics have been disturbed by post-depositional fluid flow associated
30 with Palaeozoic igneous intrusions. However, it is evident from the Ballachulish Slate
31 Formation results that anhydrous metamorphism does not disturb the Re-Os
32 geochronometer.

33

34 **Keywords:** Re-Os, Dalradian, Neoproterozoic, Sturtian, Rodinia, Laurentia

Accepted Manuscript

35 1. Introduction

36 Neoproterozoic strata record a number of significant events such as the transition
37 from stratified Proterozoic oceans with oxic surface waters and anoxic deep waters to a
38 more-or-less fully oxygenated ocean (Anbar and Knoll, 2002; Knoll, 2003; Fike et al.,
39 2006; Halverson and Hurtgen, 2007; Canfield et al., 2008). Major changes in biological
40 systems and evolutionary developments occurred towards the end of the Proterozoic
41 including the evolution of metazoans (Logan et al., 1995; 1997; Vidal and
42 Moczydlowska-Vidal, 1997; Jensen et al., 2000; Martin et al., 2000; Narbonne and
43 Gehling, 2003; Knoll et al., 2006; Macdonald, 2010a, b). Additionally, the
44 Neoproterozoic was a time of major climatic fluctuation with a number of extreme glacial
45 events recorded in the rock record (e.g. the “Snowball Earth” of Kirschvink, 1992;
46 Hoffman et al., 1998; Hoffman and Schrag, 2002 or the “Slushball Earth” of Hyde et al.,
47 2000). However, there is at present, no consensus as to the cause, extent, duration or
48 number of these glacial events (Kennedy et al., 1998; Evans, 2000; Fairchild and
49 Kennedy, 2007). The lack of precise and accurate geochronological data has severely
50 hindered attempts to develop a chronological framework for the Neoproterozoic. In
51 particular, understanding and constraining the extent and duration of these glacial events
52 has relied upon lithostratigraphy and chemostratigraphy with only a few glaciogenic
53 successions constrained by robust geochronological data (Hoffmann et al., 2004; Zhou et
54 al., 2004; Kendall et al., 2004; 2006; 2009a; Condon et al., 2005; Bowring et al., 2007;
55 Macdonald et al., 2010a).

56 During the Neoproterozoic, the continental masses of Laurentia, Baltica and
57 Amazonia were juxtaposed as a result of various orogenic events to form the
58 supercontinent Rodinia (e.g. Li et al., 2008 and references therein). During the break-up
59 of Rodinia which commenced at ca. 750 Ma there was a period of intracontinental
60 extension and basin genesis along the eastern margin of Laurentia (Harris et al., 1994;
61 Soper, 1994; Cawood et al., 2007). Scotland occupied a unique position within the
62 Rodinia supercontinent lying close to the junction of the Laurentian, Baltica and
63 Amazonian continental blocks (Dalziel, 1994). The sedimentary basins that formed
64 during the formation and breakup of Rodinia are preserved in Scotland as the
65 Torridonian, Moine and Dalradian Supergroups (Anderton, 1982; 1985; Rainbird et al.,
66 2001; Strachan et al., 2002; Cawood et al., 2003; 2004; 2007).

67 The Dalradian Supergroup of Scotland and Ireland is a metasedimentary
68 succession that was deposited on the eastern margin of Laurentia during the late
69 Neoproterozoic and Early Cambrian. Existing constraints imply the base is younger than
70 800 Ma and it extends to at least 510 Ma (Harris et al., 1994; Smith et al., 1999; Prave et
71 al., 2009a). Despite its importance in regional and global studies of the Proterozoic, our
72 understanding of the Dalradian sequence suffers from a lack of radiometric ages
73 (Halliday et al., 1989; Dempster et al., 2002). In an attempt to improve the
74 chronostratigraphy of the Dalradian, several workers have applied lithostratigraphic and
75 chemostratigraphic tools with varying levels of success (Prave, 1999; Brasier and Shields,
76 2000; Condon and Prave, 2000; Thomas et al., 2004; McCay et al., 2006; Prave et al.,
77 2009a; Sawaki et al., 2010). These studies have improved our knowledge of the
78 Proterozoic ocean chemistry and the environmental conditions of deposition within the
79 Dalradian sedimentary basin. However, chemostratigraphic tools cannot provide absolute
80 ages and ultimately rely upon correlation with sequences which have robust radiometric
81 and / or biostratigraphic age constraints (Melezhik et al., 2001; 2007; Fairchild and
82 Kennedy, 2007; Jiang et al., 2007; Meert, 2007; Giddings and Wallace, 2009; Frimmel,
83 2010). As a result, obtaining precise and accurate radiometric ages remain a priority for
84 resolving many of the issues regarding global correlations.

85 The rhenium-osmium (Re-Os) geochronometer has been shown to provide robust
86 depositional ages even for sedimentary rocks that have experienced hydrocarbon
87 maturation, greenschist metamorphism and flash pyrolysis associated with igneous
88 intrusions (Creaser et al., 2002; Kendall et al., 2004; 2006; 2009a, b; Selby and Creaser,
89 2005; Rooney et al., 2010). Thus, the Re-Os system represents an accurate, precise and
90 reliable geochronometer for providing depositional age data for the Dalradian
91 metasediments and constructing a chronostratigraphic framework for the
92 chemostratigraphic, tectonostratigraphic and lithostratigraphic datasets.

93 Here, we present new Re-Os age that constrain the depositional age of a
94 sedimentary unit from the Dalradian Supergroup. The Re-Os data also provides an
95 estimate for the osmium isotope composition of seawater in the Dalradian basin during
96 the Neoproterozoic and ultimately provide a maximum depositional age for a key
97 Neoproterozoic glacial horizon. A further aspect of this study involves the application of
98 Re-Os geochronology to sedimentary units with low Re and Os abundances (<1 ppb Re

99 and <50 ppt Os) to provide accurate and precise geochronology. Additionally, this work
100 presents results from a sedimentary unit (Leny Limestone Formation) in which the Re-Os
101 geochronometer has been disturbed as a result of post-depositional fluid flow. The results
102 from this study provide us with new insights into the robustness of the Re-Os
103 geochronometer.

104

105 **2. Geological Setting**

106 *2.1. The Dalradian Supergroup*

107 The Dalradian Supergroup of Scotland and Ireland consists of a thick (~25 km)
108 metasedimentary succession and a minor amount of mafic volcanics deposited on the
109 eastern margin of the Laurentian craton during the Neoproterozoic to Early Cambrian
110 (Fig. 1; Harris et al., 1994 and references therein). This quoted thickness of the Dalradian
111 Supergroup is a cumulative thickness from all subgroups and is not a true reflection of
112 sediment thickness. Many aspects of basin genesis have proved controversial, with little
113 consensus apparent even after more than a century of studies. Most models for Dalradian
114 deposition invoke a long, shallow-marine, ensialic basin which underwent prolonged
115 extension during the late Neoproterozoic, resulting in the eventual separation of Laurentia
116 from western Gondwana at ca. 550 Ma (Hoffman, 1991; Soper, 1994; Dalziel and Soper,
117 2001). An alternative model proposes that the lower portions of the Dalradian represented
118 a rapidly formed foredeep basin associated with the mid-Neoproterozoic (840 – 730 Ma)
119 Knoydartian Orogeny (Prave, 1999). In both models extensional tectonics played a major
120 role in the genesis of the upper portions of the Dalradian basin during the latest
121 Neoproterozoic to Early Cambrian.

122 Lithostratigraphic correlation of the Dalradian Supergroup is hampered by the
123 paucity of volcanic horizons suitable for U-Pb geochronology and the lack of
124 biostratigraphically diagnostic fossils (Fig. 2). Additionally, many portions of the
125 Dalradian sequence exhibit extreme facies variability along strike having experienced
126 complex polyphase deformation and metamorphism (Harris et al., 1994, Strachan et al.,
127 2002 and references therein). Despite these issues, a coherent lithostratigraphy has been
128 established from western Ireland to the Shetland Islands, 200 km north of mainland
129 Scotland (Harris et al., 1994).

130 The Dalradian Supergroup consists of four groups which are from oldest to
131 youngest; the Grampian, Appin, Argyll and Southern Highland groups (Figs. 1 and 2).

132 The basal Grampian Group crops out primarily in the Central Highlands although
133 possible correlatives exist on the north Grampian coast and on the Shetland Islands
134 (Strachan et al., 2002). The Grampian Group consists of up to 7 km of predominantly
135 marine, quartzo-feldspathic psammites and semi-pelites (Glover and Winchester, 1989;
136 Harris et al., 1994). The Grampian Group sedimentary succession displays sharp lateral
137 variations typical of a syn-rift origin (Soper and England, 1995; Banks et al., 2007). The
138 overlying Appin Group is exposed in a broad zone throughout Scotland and Ireland as far
139 north as the Shetland Islands. The Appin Group consists of up to 4 km of quartzite, semi-
140 pelites and phyllites deposited as a post-rift, thermal subsidence sequence (Litherland,
141 1980; Glover et al., 1995; Soper and England, 1995; Glover and McKie, 1996). The
142 overlying Argyll Group records rapid deepening of the basin following the shallow
143 marine conditions of the Appin Group (Anderton, 1985). The Argyll Group consists of a
144 thick heterogeneous succession of shelf sediments up to 9 km thick which passes upwards
145 into deep water turbidite and basinal facies and associated mafic volcanics (Anderton,
146 1982). The marked change from a shelf setting to deep water sedimentation is widely
147 ascribed to the onset of syn-depositional rifting. The basal subgroup (Islay Subgroup) of
148 the Argyll Group is marked by a distinctive and persistent tillite horizon; the Port Askaig
149 Formation, correlatives of which are traceable from Connemara in western Ireland to
150 Banffshire in NE Scotland (Anderton, 1985; Harris et al., 1994). The Southern Highland
151 Group (along with the newly defined Trossachs Group of Tanner and Sutherland, 2007)
152 marks the top of the Dalradian succession and consists of ca. 4 km of coarse-grained
153 turbiditic clastics and volcanoclastic strata (Anderton, 1985; Soper and England, 1995).
154 The Southern Highland Group is considered to represent the change from a period of
155 continental rifting and rupture to that of a thermally subsiding margin (Anderton, 1985).

156

157 *2.1.1. Glaciogenic horizons within the Dalradian and possible global* 158 *correlations*

159 The Port Askaig Formation of the Argyll Group is a thick (~900 m) succession of
160 diamictites interbedded with sandstone, conglomerate and mudstone (Kilburn et al., 1965;
161 Spencer, 1971; Eyles, 1988; Arnaud and Eyles, 2002). The formation represents the most

162 persistent and distinctive glaciogenic horizon within the Dalradian Supergroup (Fig. 2). A
163 glaciogenic origin was first recognised in the late nineteenth century (Thomson, 1871;
164 1877), and is described in detail in the classic memoir of Spencer (1971). The most
165 extensive outcrops of the Port Askaig Formation consists of ~400 m of coarse-grained
166 and poorly sorted diamictite interbedded with sandstone, mudstone and conglomerate
167 with some megaclasts in the diamictite exceeding 100 m in size (Spencer, 1971; Arnaud,
168 2004). Recent studies identified enriched $\delta^{13}\text{C}$ (+11.7‰) and unradiogenic $^{87}\text{Sr}/^{86}\text{Sr}$
169 (0.7067) in carbonate formations above and below the Port Askaig Formation (Brasier
170 and Shields, 2000; Sawaki et al., 2010). These data have been used to correlate the
171 glaciogenic horizon with the ca. 750 – 690 Ma global Sturtian glaciation (Brasier and
172 Shields, 2000; Fanning and Link, 2004; McCay et al., 2006; Macdonald et al., 2010a).
173 Two more stratigraphically limited glaciogenic units within the Dalradian Supergroup
174 have also been identified; the Stralinchy “Boulder Bed” Formation and the Inishowen -
175 Loch na Cille Ice Rafted Debris (IRD) Formations (Fig. 2; Condon and Prave, 2000;
176 McCay et al., 2006). The Stralinchy Formation occurs in the Easdale Subgroup in
177 Donegal in NW Ireland and has been correlated with the ~635 Ma global Marinoan
178 glaciation (Hoffmann et al., 2004; Condon et al., 2005; McCay et al., 2006). The Loch na
179 Cille and Inishowen glaciogenic formations occur within the uppermost Argyll Group
180 and basal Southern Highland Group respectively, and have been correlated with the 580
181 Ma Laurentian Gaskiers glacial event (Condon and Prave, 2000; Bowring et al., 2003).

182

183 2.2. Current chronological constraints for the Dalradian Supergroup

184 With the exception of *Bonnia-Ollenellus* Zone Early Cambrian trilobites and
185 inarticulate brachiopods of the upper Southern Highland Group, the Dalradian
186 Supergroup is almost entirely devoid of fossils (Pringle, 1939; Fletcher and Rushton,
187 2007). In addition, absolute chronological constraints on the age of Dalradian
188 sedimentation are also very sparse (Fig. 2). The oldest phase of volcanic activity in the
189 Dalradian Supergroup occurs within correlatives of the Port Askaig Formation in NE
190 Scotland (Chew et al., 2010). However, this thin tholeiitic pillow basalt has not been
191 dated thus far. The lower part of the Southern Highland Group in SW Scotland is
192 characterised by ca. 2 km of tholeiitic mafic volcanic rocks and sills (Tayvallich Volcanic
193 Formation). The Tayvallich Formation is cross cut by a 595 ± 4 Ma (U-Pb SHIRIMP)

194 keratophyre intrusion and a felsic tuff from this formation has yielded a U-Pb zircon age
195 of 601 ± 4 Ma (Halliday et al., 1989; Dempster et al., 2002). Pegmatites from the Central
196 Scottish Highlands has yielded a U-Pb monazite age of 806 ± 3 Ma although the
197 stratigraphic position of these pegmatites remains controversial (Noble et al., 1996).
198 These pegmatites have been suggested to intrude into Grampian Group rocks thus
199 providing a minimum age for these sediments (Noble et al., 1996; Highton et al., 1999).
200 However, other studies (e.g. Smith et al., 1999) propose that the pegmatites intrude into
201 the Dava and Glen Banchor successions which lie unconformably below the Grampian
202 Group and that therefore the Grampian Group is younger than 806 Ma (Smith et al.,
203 1999; Strachan et al., 2002).

204 Numerous studies have utilised $\delta^{13}\text{C}$, $\delta^{18}\text{O}$ and $^{87}\text{Sr}/^{86}\text{Sr}$ data from several different
205 carbonate units of the Dalradian Supergroup with the aim of correlation with global
206 chemostratigraphic curves (Brasier and Shields, 2000; Thomas et al., 2004; McCay et al.,
207 2006; Halverson et al., 2007a; Prave et al., 2009a; Sawaki et al., 2010). A composite $\delta^{13}\text{C}$
208 profile for the Dalradian Supergroup has been used to tentatively correlate the
209 Ballachulish Limestone of the Appin Group with the ca. 800 Ma Bitter Springs anomaly
210 (Prave et al., 2009a; Fig. 2). Additional correlations include the pre-Marinoan Trezona
211 anomaly and ca. 635 Ma Marinoan-equivalent cap carbonate sequence with units of the
212 middle Easdale Subgroup and the terminal Proterozoic (ca. 600 – 551 Ma) Shuram-
213 Wonoka anomaly in the Girlsta Limestone on Shetland (Melezhik et al., 2008; Prave et
214 al., 2009a, b).

215

216 *2.3. Metamorphism and deformation of the Dalradian Supergroup*

217 The Dalradian Supergroup of Scotland is one of the classic areas for the study of
218 regional and contact metamorphism (e.g., Barrow, 1893; Tilley, 1925; Baker, 1985; Voll
219 et al., 1991; Dempster et al., 1992; Pattison and Harte, 1997). The main phases of
220 regional metamorphism took place during the Grampian Orogeny. The Grampian
221 Orogeny is understood to be related to the collision of Laurentia with an oceanic arc
222 during the Early Ordovician and can be considered broadly equivalent to the Taconic
223 Orogeny of the Appalachians (Dewey and Mange, 1999; Soper et al., 1999).
224 Geochronological constraints for the Grampian Orogeny include U-Pb zircon ages from
225 syn-tectonic intrusives of 475 – 468 Ma and Sm-Nd metamorphic garnet crystallisation

226 ages of 473 – 465 Ma which date peak metamorphism (Friedrich et al., 1999; Baxter et
227 al., 2002).

228 The Dalradian sedimentary succession also experienced contact metamorphism
229 associated with the intrusion of numerous Late Caledonian (ca. 430 – 390 Ma; Oliver,
230 2001) granites throughout the Grampian Terrane of Scotland (Fig. 1). In addition to the
231 granites there are also a number of minor Late Palaeozoic intrusive suites recorded in the
232 Dalradian (Neilson et al., 2009 and references therein).

233

234 **3. Samples for this study**

235 Two localities were chosen for Re-Os geochronology analyses; the Ballachulish Slate
236 Formation from the Ballachulish Subgroup of the Appin Group and the Leny Limestone
237 Formation of the Southern Highland Group (Figs. 1 and 2). The Ballachulish Slate was
238 chosen to provide a maximum age constraint on the depositional age of the Port Askaig
239 Formation (Fig. 2). The Leny Limestone Formation was chosen as it contains the only
240 biostratigraphically diagnostic fauna found in the Dalradian Supergroup (Pringle, 1939;
241 Fletcher and Rushton, 2007). Additionally, the metasedimentary rocks of the Dalradian
242 Supergroup represent an opportunity to further our understanding of the effects of
243 regional and contact metamorphism on the Re-Os geochronometer.

244

245 *3.1. Appin Group – Ballachulish Slate Formation*

246 The Appin Group consists of three subgroups, the Lochaber, Ballachulish and Blair
247 Atholl (Fig. 2). The Ballachulish Slate Formation consists of ca. 400 m of pyritiferous
248 black slates and graphitic phyllites. Samples were collected on the eastern foreshore of
249 Loch Linnhe at the entrance to Loch Leven (56° 42. 1' N, 5° 11. 6' W; Fig. 1). In this
250 area, the top of the Ballachulish Slate Formation is estimated to be ca. 1 km below the
251 equivalent of the Port Askaig Formation (Litherland, 1980; Harris et al., 1994). Regional
252 metamorphic grade associated with the Grampian Orogeny varies from chlorite grade in
253 the NW to garnet grade in the SE. Estimates of P-T conditions range from ca. 450 - 550°
254 C from NW to SE, at ca. 6 kbar (Pattison and Voll, 1991). In addition to Grampian
255 regional metamorphism, the Ballachulish Slates also experienced Late Caledonian (ca.
256 430 Ma) igneous activity and contact metamorphism primarily associated with the well
257 characterised Ballachulish Igneous Complex (Pattison and Harte, 1997; Pattison, 2006).

258 The metamorphic aureole varies in width from ca. 400 to 1700 m, based upon the first
259 appearance of cordierite in metapelites (Pattison, 2006). Regional P-T conditions at the
260 time of intrusion are estimated at ca. 250 – 300° C at ca. 3 kbar. The age of the
261 Ballachulish Igneous Complex is constrained by Re-Os molybdenite and U-Pb zircon
262 ages of 433.5 ± 1.8 Ma and 428 ± 9.8 Ma, respectively (Conliffe et al., 2010; Rogers and
263 Dunning, 1991, recalculated by Neilson et al., 2009). Fluid flow between the intrusion
264 and the aureole was limited and there is no evidence for a large-scale hydrothermal
265 circulation system or associated mineralogical changes connected to the intrusion (Harte
266 et al., 1991; Pattison, 2006).

267 The slates analysed in this study were sampled ca. 2 km NNW of the NW contact of
268 the Ballachulish Igneous complex and are hence outside the aureole. The slates sampled
269 are black and massive with bedding occasionally still discernible and predominantly
270 orientated parallel to cleavage. X-ray diffractometry (XRD) studies indicate that the
271 Ballachulish Slates have a composition of quartz, mica, chlorite and feldspars (albite and
272 occasionally orthoclase), typical of an argillaceous slate. The samples of Ballachulish
273 slate used in this study are similar in composition to those described in greater detail by
274 Walsh (2007).

275

276 3.2. Southern Highland Group – Leny Limestone

277 The Leny Limestone forms part of the Keltie Water Grit Formation of the Southern
278 Highland Group. The formation consists of pale grey to white, siliceous grits, black
279 graphitic slates and rare locally fossiliferous limestones (Tanner and Pringle, 1999). The
280 limestones of this formation yield a fauna including polymerid and miomerid trilobites,
281 brachiopods, sponges, hyoliths and bradoriids (Fletcher and Rushton, 2007). The
282 miomerid trilobites indicate a stratigraphical age equivalent to the base of the paradoxidid
283 Amgan Stage of Siberia traditionally regarded as Middle Cambrian (511 – 506 Ma, Ogg
284 et al., 2008). However, the polymerid trilobites e.g., *Pagetides*, are forms from the
285 *Bonnia-Olenellus* Zone and are thus regarded as Lower Cambrian (516.5 – 512 Ma; Ogg
286 et al., 2008). An age of ca. 512 Ma has been adopted here as the age of the Leny
287 Limestone Formation (Fletcher and Rushton, 2007).

288 Black graphitic slates of the Leny Limestone Formation were sampled on the south-
289 easterly face of the Western Quarry (56° 15.5' N, 4° 13.1 W; Fig. 1). The metamorphic

290 grade during the Grampian Orogeny was low, with an estimated peak metamorphic
291 temperature of 270°C (Tanner and Pringle, 1999). Detrital biotite is preserved, albeit
292 commonly partially altered to chlorite. The locality is also the locus of several phases of
293 igneous activity such as intrusions of Devonian quartz-felsite dykes and Permo-
294 Carboniferous quartz dolerite dykes (British Geological Survey, 2005; Fletcher and
295 Rushton, 2007). The Devonian intrusion exhibits a 70 m fault offset, though this faulting
296 is not seen in the Permo-Carboniferous dyke suggesting faulting occurred prior to this
297 younger intrusive episode. XRD analysis of the Leny Limestone Formation slates reveal a
298 composition of quartz, micas (mainly muscovite), kaolinite and a serpentine-group
299 mineral with the chemical formula of $\text{Fe}_3\text{Si}_2\text{O}_5(\text{OH})_4$ suggested to represent berthierine
300 (Brindley, 1982).

301

302 **4. Sampling and analytical methods**

303 Sampling of the Ballachulish Slate and Leny Limestone Formations was limited
304 to a vertical interval of ca. 50 cm of stratigraphy across a lateral interval of several tens of
305 metres. Weathered material was removed from the outcrop prior to sampling of fresh
306 surfaces. Large (~100 g) samples were selected to ensure homogenisation of Re-Os
307 abundances in the samples (Kendall et al., 2009b). All samples were polished to remove
308 cutting and drilling marks to eliminate any potential contamination. The samples were
309 dried at 60 °C for ~12 hrs and then crushed to a fine powder of ~30 µm. The samples
310 were broken into chips with no metal contact and powdered in a ceramic dish using a
311 shatterbox.

312 Rhenium-osmium isotope analysis was carried out at Durham University's TOTAL
313 laboratory for source rock geochronology and geochemistry at the Northern Centre for
314 Isotopic and Elemental Tracing (NCIET). Sample digestion using a $\text{CrO}_3\text{-H}_2\text{SO}_4$ solution
315 is the preferred method for Re-Os geochronology as it has been shown to preferentially
316 liberate hydrogenous Re and Os, ultimately providing more precise ages (Selby and
317 Creaser, 2003; Kendall et al., 2004). An inverse *aqua-regia* solution was also employed
318 in an attempt to evaluate the contribution of detrital Re and Os in these samples. Previous
319 work has shown that *aqua-regia* digestion liberates both non-hydrogenous (detrital and
320 meteoritic) and hydrogenous Re and Os. This detrital Os component has been shown to
321 represent a source of geological scatter that results in determination of imprecise and / or

322 inaccurate depositional ages (Ravizza et al., 1991; Selby and Creaser, 2003; Kendall et
323 al., 2004).

324 Approximately 1 g of sample powder was digested together with a mixed tracer
325 (spike) solution of ^{190}Os and ^{185}Re in a $\text{Cr}^{\text{VI}}\text{-H}_2\text{SO}_4$ solution in a sealed carius tube at 220
326 $^\circ\text{C}$ for ~ 48 h (Selby and Creaser, 2003; Kendall et al., 2004). Through the use of the $\text{Cr}^{\text{VI}}\text{-}$
327 H_2SO_4 digestion media it is possible to preferentially liberate the hydrogenous Re and Os
328 components from the samples thus limiting any detrital component (Selby and Creaser,
329 2003; Kendall et al., 2004). For the inverse *aqua-regia* digestions approximately 1 g of
330 sample powder was dissolved together with a spike solution of ^{190}Os and ^{185}Re in a 1:2
331 acid mixture of 3 ml 12 N HCl and 6 ml of 16 N HNO_3 in a sealed carius tube at 220 $^\circ\text{C}$
332 for ~ 48 h (Selby and Creaser, 2003).

333 Rhenium and Os were purified from the acid solution using solvent extraction
334 (CHCl_3), micro-distillation and anion chromatography methods and analysed by negative
335 thermal ionisation mass spectrometry as outlined by Selby and Creaser (2003), and Selby
336 (2007). The purified Re and Os fractions were loaded onto Ni and Pt filaments,
337 respectively (Selby et al., 2007), with the isotopic measurements conducted using a
338 ThermoElectron TRITON mass spectrometer via static Faraday collection for Re and ion-
339 counting using a secondary electron multiplier in peak-hopping mode for Os. Average
340 procedural blanks for the $\text{Cr}^{\text{VI}}\text{-H}_2\text{SO}_4$ method during this study were 16.8 ± 0.06 pg and
341 0.43 ± 0.06 pg (1σ S.D., $n = 3$) for Re and Os respectively, with an average $^{187}\text{Os}/^{188}\text{Os}$
342 value of $\sim 0.25 \pm 0.11$ ($n = 3$). For the inverse *aqua-regia* method procedural blanks for
343 Re and Os were 1.9 ± 0.01 pg and 0.12 ± 0.06 pg, respectively (1σ S.D. $n = 2$) with an
344 average $^{187}\text{Os}/^{188}\text{Os}$ value of $\sim 0.4 \pm 0.5$ (1σ S.D., $n = 2$).

345 Uncertainties for $^{187}\text{Re}/^{188}\text{Os}$ and $^{187}\text{Os}/^{188}\text{Os}$ are determined by error propagation
346 of uncertainties in Re and Os mass spectrometer measurements, blank abundances and
347 isotopic compositions, spike calibrations and reproducibility of standard Re and Os
348 isotopic values using methods identical to previous studies (e.g., Kendall et al., 2004;
349 Selby and Creaser, 2005). The Re-Os isotopic data, 2σ calculated uncertainties for
350 $^{187}\text{Re}/^{188}\text{Os}$ and $^{187}\text{Os}/^{188}\text{Os}$ and the associated error correlation function (ρ) are
351 regressed to yield a Re-Os date using *Isoplot V. 3.0* with a λ ^{187}Re constant of 1.666×10^7
352 a^{-1} (Ludwig, 1980; Smoliar et al., 1996; Ludwig, 2003).

353 To ensure and monitor long-term mass spectrometry reproducibility, in-house
354 standard solutions of Re and Os (Durham Romil Osmium Standard [DROsS]) are
355 repeatedly analysed at NCIET. The Re standard analysed during the course of this study
356 is made from 99.999% zone-refined Re ribbon and is considered to have an identical Re
357 isotopic composition to that of the AB-1 Re standard (Creaser et al., 2002; Selby and
358 Creaser, 2003; Kendall et al., 2004). The NCIET Re standard yields an average
359 $^{185}\text{Re}/^{187}\text{Re}$ ratio of 0.59772 ± 0.00172 (1 SD, $n = 114$). This is in excellent agreement
360 with the value reported for the AB-1 standard (Creaser et al., 2002). The Os isotope
361 reference material (DROsS) yields an $^{187}\text{Os}/^{188}\text{Os}$ ratio of 0.106093 ± 0.00015 (1 SD, $n =$
362 36). The isotopic compositions of these solutions are identical within uncertainty to those
363 reported by Rooney et al. (2010) and references therein.

364

365 5. Results

366 5.1. Ballachulish Slate Formation samples

367 The Ballachulish Slate samples have Re (0.3 – 1.9 ppb) and Os (25.5 – 52.2 ppt)
368 abundances that are close to or less than that of average continental crustal values of ~1
369 ppb and 50 ppt, respectively (Table 1; Esser and Turekian, 1993; Peucker-Ehrenbrink and
370 Jahn, 2001; Hattori et al., 2003; Sun et al., 2003). The $^{187}\text{Re}/^{188}\text{Os}$ ratios range from 56.5
371 to 311.7 and the $^{187}\text{Os}/^{188}\text{Os}$ ratios range from 1.660 – 4.478 (Table 1). Regression of the
372 Re-Os isotope data yields a Re-Os age of 659.6 ± 9.6 Ma (2σ , $n = 5$, Model 1, Mean
373 Square of Weighted Deviates [MSWD] = 0.01, initial $^{187}\text{Os}/^{188}\text{Os} = 1.04 \pm 0.03$; Fig. 3a).

374 Digestion of the Ballachulish samples using inverse *aqua-regia* yields elemental
375 abundances of 0.3 – 1.8 ppb and 30.6 – 53.5 ppt for Re and Os, respectively, which are
376 identical within uncertainty to the values from the samples digested using $\text{CrO}_3\text{-H}_2\text{SO}_4$
377 (Table 1). The $^{187}\text{Re}/^{188}\text{Os}$ ratios range from 41.4 to 308.2 and the $^{187}\text{Os}/^{188}\text{Os}$ ratios range
378 from 1.472 to 4.364 (Table 1). Regression of the aqua regia derived Re-Os isotope data
379 yields a Model 3 age of 655 ± 49 Ma (2σ , $n = 5$, MSWD = 16) with an initial Os isotope
380 composition of 1.03 ± 0.16 (Fig. 3b).

381

382 5.2. Leny Limestone slate samples

383 The Leny Limestone slates are enriched in Re (46.2 – 66.1 ppb) and Os (419 – 633
384 ppt) in comparison to average continental crustal values of ~1 ppb and 50 ppt,

385 respectively (Table 1). The $^{187}\text{Re}/^{188}\text{Os}$ ratios range from 898.4 to 1228.0 and the
386 $^{187}\text{Os}/^{188}\text{Os}$ ratios range from 6.162 – 8.075 (Table 1). Regression of the Re-Os isotope
387 data yields a Re-Os age of 310 ± 110 Ma (2σ , $n = 9$, Model 3, MSWD = 388, initial
388 $^{187}\text{Os}/^{188}\text{Os} = 1.7 \pm 2.0$; Fig. 4).

389

390 **6. Discussion**

391 *6.1. Effect of non-hydrogenous Re and Os in low abundance samples*

392 The $\text{CrO}_3\text{-H}_2\text{SO}_4$ method has been shown to yield precise and accurate
393 depositional age determinations for both Phanerozoic and Proterozoic sedimentary
394 successions (Kendall et al., 2004; 2006; 2009a, c; Selby and Creaser, 2005; Anbar et al.,
395 2007; Selby, 2007; Yang et al., 2009; Rooney et al., 2010). Data from the Ballachulish
396 samples using the $\text{CrO}_3\text{-H}_2\text{SO}_4$ digestion method yields a Model 1 age with a low
397 uncertainty (1.5 %) and a low degree of scatter about the isochron (MSWD <1).
398 However, as these samples have Re and Os abundances comparable to that of average
399 continental crust it is important to assess the effects of a detrital Re and Os component on
400 the geochronology data. It has been shown that the incorporation of a detrital Os
401 component could lead to a younger or older age depending on the isotopic composition of
402 the detrital Os (Ravizza et al., 1991). The effects of a detrital Os component on Re-Os
403 depositional ages have been assessed previously during the development of the $\text{CrO}_3\text{-}$
404 H_2SO_4 method (Selby and Creaser, 2003; Kendall et al., 2004).

405 The results from the inverse *aqua-regia* digestion show Re and Os abundances
406 that are comparable with the samples digested using $\text{CrO}_3\text{-H}_2\text{SO}_4$ (Table 1). The isotopic
407 composition data highlights the impact of detrital Re and Os on the determination of
408 depositional ages. All of the $^{187}\text{Re}/^{188}\text{Os}$ and $^{187}\text{Os}/^{188}\text{Os}$ values for the *aqua-regia*
409 samples are lower than those of the samples digested using $\text{CrO}_3\text{-H}_2\text{SO}_4$ (15% and 9%
410 lower, respectively; Table 1). This suggests that the *aqua-regia* digestion has liberated an
411 unradiogenic detrital Os component. Both ages for the Ballachulish Slate Formation are
412 very similar however, however the *aqua-regia* Re-Os data set have a much larger degree
413 of scatter (MSWD = 16) and yield a less precise age (9% uncertainty; Fig 3b, c). The
414 samples digested using the $\text{CrO}_3\text{-H}_2\text{SO}_4$ method yield a much more precise age with a
415 lower degree of scatter (MSWD = 0.01; Fig. 3a). These variations in precision and
416 geological scatter are very similar to those identified by previous studies which undertook

417 digestion of samples in *aqua-regia* (Selby and Creaser, 2003; Kendall et al., 2004).
418 Additionally, digesting samples in the $\text{CrO}_3\text{-H}_2\text{SO}_4$ solution at 80 °C instead of 220 °C
419 has been shown to yield identical data supporting the notion that this method does not
420 liberate non-hydrogenous Re and Os even at high temperatures (Kendall et al., 2009a).

421 The $^{187}\text{Os}/^{188}\text{Os}$ initial ratio (Os_i) data from the samples digested using the $\text{CrO}_3\text{-}$
422 H_2SO_4 method are all very similar with a coefficient of variation of 0.3% in contrast to
423 the Os_i data from the samples digested in *aqua-regia* which have a coefficient of
424 variation of 5% (coefficient of variation = $(\text{SD}/\text{mean}) \times 100$; Table 1). This suggests that
425 there were variations in Os isotope composition and / or magnitude of the detrital Os flux
426 into the Ballachulish Slate during deposition. Again, this is identical to the findings of
427 Kendall et al. (2004) on the Old Fort Point Formation of Canada.

428 The low degree of scatter coupled with the precise age of 659.6 ± 9.6 Ma
429 represents a depositional age for the Ballachulish Slate Formation and the initial
430 $^{187}\text{Os}/^{188}\text{Os}$ isotope composition of 1.04 represents that of seawater at the time of
431 deposition.

432

433 *6.2. Implications for low Re and Os abundance geochronology*

434 The Re-Os age for the Ballachulish Slate Formation indicate that samples with low
435 Re and Os abundances (<1 ppb Re and <50 ppt Os) can be used to provide precise
436 geochronological data (Fig. 3a; Table 1). These values are similar to abundances in
437 average continental crust which range from 0.2 – 2 ppb and 30 – 50 ppt, respectively
438 (Esser and Turekian, 1993; Peucker-Ehrenbrink and Jahn, 2001; Hattori et al., 2003; Sun
439 et al., 2003).

440 Previous work on Re-Os geochronology has focused on sedimentary units greatly
441 enriched in Re and Os with abundances >20 ppb and 500 ppt, respectively (Ravizza et al.,
442 1989; Cohen et al., 1999, Creaser et al., 2002; Selby and Creaser, 2005; Selby, 2007;
443 Rooney et al., 2010). However, some recent studies have successfully applied the Re-Os
444 geochronometer to sedimentary rocks with low to moderate enrichments of Re and Os
445 (1.7 – 50 ppb and 82 – 250 ppt, respectively; Kendall et al., 2004; 2006; 2009a, b; Yang
446 et al., 2009). The Re-Os geochronology data for the Ballachulish Slate Formation
447 represent successful application of the system to samples with very low Re and Os
448 abundances provided that the system has not been disturbed as discussed below.

449 The low Re and Os abundances do not appear to impair the robustness of the system
450 as the Ballachulish samples all have similar $^{187}\text{Os}/^{188}\text{Os}$ (Os_i) values, yield a large spread
451 in present-day $^{187}\text{Re}/^{188}\text{Os}$ values (~ 260 units) and display positively correlated,
452 radiogenic $^{187}\text{Os}/^{188}\text{Os}$ values indicative of a closed system (Table 1). This positive
453 correlation indicates that the 659.6 ± 9.6 Ma age for the Ballachulish Slate Formation
454 does not represent a mixing line. Additionally, if the systematics had been disturbed, any
455 detrital Os component in these samples would represent a significant cause of geological
456 uncertainty, resulting in an imprecise and geologically meaningless age. The highly
457 precise age coupled with the low degree of scatter in the data, (659.6 ± 9.6 and $\text{MSWD} =$
458 0.01), suggests that this is a depositional age and the Os_i value of 1.04 represents the Os
459 isotope composition of local seawater at the time of deposition. The results from the
460 Ballachulish Slate Formation strongly suggest that the system can be applied to
461 sedimentary units that have low Re and Os abundances. From this we can also propose
462 that the system is robust enough to provide depositional ages for strata that have
463 experienced complex and polyphase metamorphic histories.

464

465 6.3. Age of the Ballachulish Slate Formation

466 The Re-Os isotope data from the Ballachulish slates yield an age of 659.6 ± 9.6 Ma
467 which represents the depositional age of the Ballachulish Slate Formation (Fig. 3a).
468 Accordingly, this Re-Os age defines a maximum age constraint for the glaciogenic Port
469 Askaig Formation (Fig. 2). Taken in the context of the previous geochronological
470 constraints for the Dalradian, the Re-Os age for the Ballachulish Slate Formation strongly
471 suggests that the Argyll Group was deposited within ~ 60 Ma, prior to the eruption of the
472 Tayvallich volcanics at ca. 600 Ma. From these two geochronological constraints,
473 combined with the possibility that correlatives of the ca. 635 Ma Marinoan cap carbonate
474 sequence are found within units of the Easdale Subgroup (McCay et al., 2006) we suggest
475 that the Port Askaig Formation records a low latitude glacial event that occurred at ca.
476 650 Ma.

477 Much of the recent work relating to the Dalradian Supergroup has focused on $\delta^{13}\text{C}$
478 carbonate and $^{87}\text{Sr}/^{86}\text{Sr}$ chemostratigraphy of the various carbonate units (Prave et al.,
479 2009a and references therein; Sawaki et al., 2010). This focus on chemostratigraphy
480 coupled with the lack of reliable geochronology data has resulted in several attempts at

481 correlation of the Dalradian Supergroup with better constrained Neoproterozoic
482 sequences (McCay et al., 2006; Prave et al., 2009a; Sawaki et al., 2010). The Ballachulish
483 Limestone is ca. 200 m in thickness and passes upwards into the Ballachulish Slate
484 (Anderton, 1982; Prave et al., 2009a). Work by Prave et al. (2009a) suggested that the
485 Ballachulish Limestone possess $\delta^{13}\text{C}_{\text{carbonate}}$ values as low as -7‰ and was tentatively
486 correlated with the ca. 800 Ma Bitter Springs anomaly of central Australia (Hill and
487 Walter, 2000; Halverson et al., 2007b). However, the Re-Os data of 659.6 ± 9.6 Ma for
488 the Ballachulish Slate Formation negates the possibility of this correlation (Fig. 2).

489 A 60 Ma duration for Argyll Group deposition suggested by the Re-Os data presented
490 here contrasts with a duration of ca. 120 Ma required by chemostratigraphic and
491 lithostratigraphic correlations of the Port Askaig Formation with a ca. 715 Ma “Sturtian”
492 glacial (Prave, 1999; Brasier and Shields, 2000; Prave et al., 2009a;). A short duration for
493 Argyll Group deposition is geologically more probable given that the Argyll Group
494 represents a time of increased tectonic activity and syn-depositional faulting with rapid
495 deposition taking place in subsiding fault-bounded sub-basins (Anderton, 1982; 1985). A
496 short duration for Argyll Group deposition also negates the need for any putative
497 regional-scale unconformity within the Argyll Group, which remains contentious (see
498 Hutton and Alsop, 2004 and Tanner et al., 2005 for a review).

499 The new Re-Os geochronology data provide a more precise chronostratigraphic
500 framework for understanding the tectonic evolution of the Dalradian basin and the onset
501 of sedimentation within the basin. Furthermore, the Re-Os geochronology helps refine
502 Neoproterozoic palaeogeographies related to the formation and breakup of the Rodinia
503 supercontinent (e.g., Li et al., 2008; Li and Evans, 2010). Deposition of the Dalradian
504 Supergroup occurred along the eastern margin of Laurentia, close to the triple junction of
505 Baltica, Laurentia and Amazonia (Soper, 1994; Dalziel, 1994).

506

507 *6.4. Implications for global correlations involving the glacial Port Askaig Formation*

508 At present, global correlation schemes for Neoproterozoic glaciogenic deposits are
509 dependent on correlation of two distinctive types of diamictite cap-carbonate pairs. These
510 have been designated as “Sturtian” and “Marinoan” events after the type localities in
511 southern Australia (Kennedy et al., 1998; Hoffman and Schrag, 2002; Halverson et al.,
512 2005; Corsetti and Lorentz, 2006). The Sturtian glaciation however, is also used to define

513 much older glacial events than the Sturtian *sensu stricto* of the Adelaide Rift Complex
514 which has geochronological constraints of ca. 640 – 660 Ma (Preiss, 2000; Kendall et al.,
515 2009a and references therein). These earlier glacial events assigned to the “Sturtian” have
516 geochronological constraints which indicate low-latitude global glaciation at ca. 715 Ma
517 based on U-Pb zircon ages (Bowring et al., 2007; Macdonald et al., 2010a). In this
518 summary, they are referred to as middle Cryogenian (ca. 715 Ma) deposits to distinguish
519 them from younger Sturtian (*sensu stricto*) glacial deposits on the Australian craton at ca.
520 640 – 660 Ma.

521 Early work on correlation of the Port Askaig Formation (Fig. 2) suggested a possible
522 correlation with North Atlantic Varangerian tillite sequences which were originally
523 constrained by a Rb-Sr diagenetic illite age of ca. 630 Ma (Hambrey, 1983; Fairchild and
524 Hambrey, 1995; Gorokhov et al., 2001). Correlation of the Port Askaig Formation with
525 the Varangerian tillite was also suggested by $^{87}\text{Sr}/^{86}\text{Sr}$ chemostratigraphy of Dalradian
526 limestones that indicate that the base of the Dalradian Supergroup is younger than ca. 800
527 Ma and may be as young as ca. 700 Ma (Thomas et al., 2004). This correlation is difficult
528 to support as the geochronological constraints for the Varangerian glaciation are based
529 upon Rb-Sr illite geochronology, which is unlikely to represent a depositional age
530 (Morton and Long, 1982; Ohr et al., 1991; Awwiller, 1994; Evans, 1996; Gorokhov et al.,
531 2001; Selby, 2009).

532 Recent work has rejected the correlation of the Port Askaig Formation and the
533 Varangerian glaciation. Instead, $\delta^{13}\text{C}$ and $^{87}\text{Sr}/^{86}\text{Sr}$ profiles from the underlying Islay
534 Limestone and overlying Bonahaven Formation have been used to suggest a middle
535 Cryogenian (ca. 715 Ma) age for the Port Askaig Formation (Brasier and Shields, 2000;
536 Prave et al., 2009a). Further ‘evidence’ for a 715 Ma middle Cryogenian age for the Port
537 Askaig Formation is the presence of younger glaciogenic units in the Dalradian, namely
538 the Stralinchy-Reelan (a possible Marinoan correlative) and the Inishowen-Loch na Cille
539 Formations (a possible Gaskiers correlative; Condon and Prave, 2000; McCay et al.,
540 2006). However, the Re-Os age of 659.6 ± 9.6 Ma for the Ballachulish Slate Formation
541 refutes the notion that the Port Askaig Formation is a component of a middle Cryogenian
542 (ca. 715 Ma) glaciation. As reported above, the Re-Os age, coupled with existing
543 geochronology constraints on the Tayvallich volcanics strongly suggest that the Port
544 Askaig Formation records a glacial event on the eastern margin of Laurentia at ~650 Ma.

545 Palaeomagnetic constraints from Laurentia during the Neoproterozoic indicate that
546 Laurentia (and hence the Port Askaig Formation) was at low latitudes from 723 – 614 Ma
547 (see Trinidade and Macouin, 2007 and references therein). Similarly, the Sturtian (*sensu*
548 *stricto*) glaciations on the Australian craton were also at low latitude and Re-Os
549 geochronology of post-glacial rocks indicates an age of ~650 Ma for these glacial
550 deposits. The Ballachulish Slate Formation Re-Os geochronology implies that the Port
551 Askaig Formation could be correlated with the ~650 Ma Sturtian (*sensu stricto*) deposits
552 of the Adelaide Rift Complex (Preiss, 2000; Kendall et al., 2006; 2009a). This suggestion
553 is also supported by the Os_i data for the Ballachulish Slate, Upper Black River Dolomite
554 and Tapley Hill formations as discussed below (Fig. 5; Kendall et al., 2006; 2009a; This
555 study).

556

557 6.5. *Os isotopic composition of seawater at 660 Ma*

558 The initial Os_i values determined from the regression of the Re-Os isotope data
559 (Table 1; Figs. 3 and 4) are interpreted to reflect the Os isotope composition of seawater
560 at the time of deposition (Ravizza and Turekian, 1989; Cohen et al., 1999; Selby and
561 Creaser, 2003). The Os isotope composition for seawater at the time of deposition of the
562 Ballachulish Slate (1.04 ± 0.03) is identical, within uncertainty, to that of the present day
563 Os isotopic composition of seawater (~1.06; Peucker-Ehrenbrink and Ravizza, 2000 and
564 references therein; Rooney et al., unpublished data). The radiogenic Os_i value from the
565 Ballachulish Slate Formation suggests that the contribution of radiogenic Os from
566 riverine inputs and weathering of upper continental crustal material (present-day riverine
567 inputs of $^{187}Os/^{188}Os \sim 1.5$; Levasseur et al., 1999) dominated over the influx of
568 unradiogenic Os from cosmic dust and hydrothermal alteration of oceanic crust and
569 peridotites (present-day $^{187}Os/^{188}Os \sim 0.13$; Walker et al., 2002a, b).

570 The radiogenic values for the Os_i of the Ballachulish Slate Formation closely
571 match values for the post-glacial Upper Black River Dolomite, Aralka and Tapley Hill
572 Formations of southern Australia (1.04; 1.00; 0.82; 0.95, respectively; Kendall et al.,
573 2006; 2009a). Although there are many contrasting palaeomagnetic reconstructions of the
574 Laurentian and Australian cratons, most models indicate that during the Neoproterozoic
575 these two cratons were both located at low latitudes and were separated by oceanic basins
576 that formed as a result of rifting associated with the breakup of Rodinia (Li et al., 2008

577 and references therein; Li and Evans, 2010). We postulate that the very similar Os_i values
578 reported from the pre-glacial Ballachulish and post-glacial Upper Black River Dolomite,
579 Aralka and Tapley Hill Formations represent a possibly global Os isotope composition
580 for the 660 – 640 Ma time interval (Kendall et al., 2006; 2009a). Additionally, this
581 ‘global’ isotope composition for this interval is significantly more radiogenic than values
582 for Mesoproterozoic seawater Os isotope composition (1.04 compared to 0.33 and 0.29;
583 Rooney et al., 2010 and Kendall et al., 2009c). One possibility is that falling sea levels
584 and the exposure of rifted margins associated with the breakup of Rodinia would expose
585 older, more radiogenic continental crust to weathering. A further explanation for the
586 increase in $^{187}Os/^{188}Os$ isotope composition for the Neoproterozoic is the increased
587 oxygenation of deep waters during the late Neoproterozoic (Canfield and Teske, 1996;
588 Anbar and Knoll, 2002; Canfield et al., 2007; 2008; Scott et al., 2008). This oxygenation
589 of the oceans and atmosphere would result in increased chemical weathering of
590 continental crust which, coupled with the breakup of Rodinia may result in an increase in
591 seawater Os as seen for the Sr isotope composition of Neoproterozoic seawater (Jacobsen
592 and Kaufman, 1999; Halverson et al., 2007a).

593

594 *6.6. Systematics of Re-Os in Leny Limestone Formation*

595 Although the Ballachulish Slate Formation experienced complex and polyphase
596 metamorphism, these samples yield a precise depositional age with a low degree of
597 scatter about the linear regression of the Re-Os data (659.6 ± 9.6 Ma, MSWD = 0.01).
598 The results for the Ballachulish Slate samples imply that anhydrous metamorphism and
599 dehydration reactions do not adversely affect Re-Os systematics. In contrast, the Leny
600 Limestone Formation which has also experienced regional Grampian metamorphic events
601 has been disturbed. We suggest that this Re-Os isotope disturbance is probably related to
602 hydration and fluid-flow events associated with Carboniferous / Permian contact
603 metamorphism as discussed below.

604 The Re-Os isotope data for the Leny Limestone Formation yield a highly imprecise
605 age of 310 ± 110 Ma (MSWD = 338) that is significantly younger than the accepted age
606 of ca. 512 Ma based upon the trilobite fauna found in the Leny Limestone (Fletcher and
607 Rushton, 2007). In addition, the Os_i value of 1.7 ± 2.0 is much more radiogenic than
608 known values for Cambrian seawater (~ 0.8 ; Mao et al., 2002) and all of the Phanerozoic.

609 The Re-Os geochronometer has been shown to be robust following hydrocarbon
610 maturation events, greenschist-facies metamorphism and flash pyrolysis thus suggesting
611 the system is robust even after temperatures as high as 650 °C and pressures as high as 3
612 kbar (Creaser et al., 2002; Kendall et al., 2004; 2006; 2009; Rooney et al., 2010).
613 Disturbance of the Re-Os systematics by chemical weathering has been identified from
614 outcrop studies on the Ohio Shale (Jaffe et al., 2002). The Leny Limestone Formation
615 outcrop is not significantly weathered and the samples were taken in such a way as to
616 avoid the effects of recent chemical weathering on the outcrop. The measures undertaken
617 to ensure that fresh samples were used for Re-Os geochronology include; removal of
618 surficial weathering prior to sampling of large (~200 g) samples extracted from the
619 outcrop prior to cutting which meant that any evidence of weathering e.g., iron-staining
620 or leaching and features such as quartz veins could be scrupulously avoided. Thus we do
621 not consider these factors to have played a role in the Re-Os analysis of the Leny
622 Limestone Formation.

623 Recent work has shown that the Re-Os geochronometer is susceptible to disturbance
624 caused by hydrothermal fluid interaction with sedimentary units associated with the
625 formation of a SEDEX deposit (Kendall et al., 2009c). The proximity of the Leny
626 Limestone exposures to the Devonian and Permo-Carboniferous intrusions and associated
627 interactions with hydrothermal fluids are likely causes of disturbance of the Re-Os
628 systematics. In agreement with work by Kendall et al. (2009c) we suggest that the Re-Os
629 age for the Leny Limestone represents a disturbed dataset. The negative Os_i values
630 calculated at 512 Ma and the anomalously young age can be best explained by post-
631 depositional mobilization of Re and Os resulting from hydrothermal fluid flow driven by
632 the igneous intrusions found within the Leny Quarry. Possibly oxidising fluids generated
633 by the intrusions may have leached Re and/or Os from the Leny Slate samples. The Leny
634 Limestone slate samples all have $^{187}Re/^{188}Os$ values that plot to the right of the 512 Ma
635 reference line suggestive of either Re gain or Os loss (Fig. 5). The occurrence of
636 kaolinite, muscovite and berthierine from XRD analysis of the Leny Limestone
637 Formation slates suggests that these minerals are the products of retrograde reactions
638 involving chlorite, muscovite and an Fe-rich phase such as cordierite that was driven by
639 reactions with hydrothermal fluids (Slack et al., 1992; Abad et al., 2010).

640 The lack of documented mineralisation (small [<1 cm thick] dolomite veins in the
641 limestones notwithstanding) and identifiable accessory or index minerals renders it
642 extremely challenging to gain a full understanding of the P-T conditions of contact
643 metamorphism in the Leny Limestone Formation. However, given that the Grampian
644 Orogeny would have generated local greenschist-facies conditions it is likely that
645 hydrothermal fluid flow driven by the Palaeozoic igneous intrusions hydrated the Leny
646 Limestone slates resulting in retrograde reactions and the disturbance of the Re-Os
647 geochronometer.

648

649 **7. Conclusions**

650 New Re-Os geochronology for the Ballachulish Slate Formation yields a depositional
651 age of 659.6 ± 9.6 Ma providing a maximum age constraint for the overlying glaciogenic
652 Port Askaig Formation. The precise age coupled with the excellent linear fit of the Re-Os
653 isotope data for the Ballachulish Slate Formation represents the first successful
654 application of the Re-Os system in samples with Re and Os abundances comparable with,
655 or lower than, average continental crustal values. Additionally, these results strongly
656 suggest that meaningful Re-Os geochronology data can be obtained from sedimentary
657 successions that have experienced polyphase contact and regional metamorphism
658 provided that thermal alteration was anhydrous.

659 The Re-Os geochronology presented here indicates that the Port Askaig Formation is
660 much younger than the middle Cryogenian glacial horizons bracketed at ca. 750 – 690
661 Ma, with which it was previously correlated. The new geochronology data for the
662 Ballachulish Slate Formation also refutes a correlation of the underlying Ballachulish
663 Limestone Formation with the ca. 800 Ma Bitter Springs anomaly of Australia (Hill and
664 Walter, 2000; Halverson et al., 2007b; Prave et al., 2009a). The Re-Os geochronology
665 provides a chronostratigraphic framework that indicates deposition of the Argyll Group
666 occurred within a ~ 60 Ma interval prior to eruption of the Tayvallich Volcanics. The Re-
667 Os data provide further support for the argument that Re-Os and U-Pb zircon
668 geochronology are fundamental if we are to use chemostratigraphy to evaluate
669 Neoproterozoic environments.

670 The Os_i value for seawater at the time of deposition of the Ballachulish Slate
671 Formation is similar to that of the present-day value indicating that the dominant input of

672 Os to seawater was radiogenic input from the weathering of the continental crust.
673 Additionally, the close similarity of Os_i values from the Ballachulish Slate Formation
674 with Sturtian (*sensu stricto*) deposits from the Australian craton indicates that the
675 dominant source of Os to the oceans was from weathering of an evolved upper
676 continental crust.

677 Disturbance of Re-Os systematics in the Leny Limestone Formation is evident by a
678 very imprecise and inaccurate age along with a negative value for the Os_i value
679 (calculated at 512 Ma) for seawater in this biostratigraphically constrained Cambrian
680 unit. These factors strongly suggest that the Re-Os system was disturbed in response to
681 hydrothermal fluid flow associated with the intrusion of a number of igneous bodies
682 during the Palaeozoic. The circulation of fluids through the Leny Limestone Formation is
683 suggested to be the cause for the gain of Re and / or the loss of Os thus generating an
684 imprecise age younger than the known depositional age.

685

686 **Acknowledgements**

687 This research was funded by a TOTAL CeREES PhD scholarship awarded to
688 ADR. Maggie White is thanked for her assistance with the XRD work. We would like to
689 thank Rob Strachan, Tony Prave, and Alex Finlay for discussions on Dalradian geology
690 and Re-Os systematics. Constructive criticism from Graham Shields and an anonymous
691 reviewer also further improved this manuscript. The TOTAL laboratory for source rock
692 geochronology and geochemistry at NCIET is partly funded by TOTAL.

693 **References:**

- 694 Abad, I., Murphy, B., Nieto, F., Guitierrez-Alonso, G., 2010. Diagenesis to
695 metamorphism transition in an episutural basin: the late Paleozoic St. Mary's
696 Basin, Nova Scotia, Canada. *Canadian Journal of Earth Sciences*, **47**, 121-135.
- 697 Anbar, A. D., Knoll, A. H., 2002. Proterozoic ocean chemistry and evolution: A
698 bioinorganic bridge? *Science* **297**, 1137-1142.
- 699 Anbar, A.D., Duan, Y., Lyons, T.W., Arnold, G.L., Kendall, B., Creaser, R.A., Kaufman,
700 A.J., Gordon, G.W., Scott, C., Garvin, J., Buick, R. 2007. A whiff of oxygen
701 before the Great Oxidation Event? *Science*, **317**, 1903 - 1906.
- 702 Anderton, R., 1982. Dalradian deposition and the late Precambrian-Cambrian history of
703 the N Atlantic region: a review of the early evolution of the Iapetus Ocean.
704 *Journal of the Geological Society* **139**, 421-431.
- 705 Anderton, R., 1985. Sedimentation and tectonics in the Scottish Dalradian. *Scot J Geol*
706 **21**, 407-436.
- 707 Arnaud, E., Eyles, C. H., 2002. Catastrophic mass failure of a Neoproterozoic glacially
708 influenced continental margin, the Great Breccia, Port Askaig Formation,
709 Scotland. *Sedimentary Geology* **151**, 313-333.
- 710 Arnaud, E., 2004. Giant cross-beds in the Neoproterozoic Port Askaig Formation,
711 Scotland: implications for snowball Earth. *Sedimentary Geology* **165**, 155-174.
- 712 Awwiller, D.N., 1994 Geochronology and Mass-Transfer in Gulf-Coast Mudrocks
713 (South-Central Texas, USA) - Rb-Sr, Sm-Nd and Ree Systematics. *Chemical*
714 *Geology*, **116**, 61-84.
- 715 Baker, A. J., 1985. Pressures and temperatures of metamorphism in the eastern Dalradian.
716 *Journal of the Geological Society* **142**, 137-148.
- 717 Banks, C.J., Smith, M., Winchester, J.A., Horstwood, M.S.A., Noble, S.R., Ottley, C.J.,
718 2007. Provenance of intra-Rodinian basin-fills: The Lower Dalradian Supergroup,
719 Scotland. *Precambrian Research* **153**, 46-64.
- 720 Barrow, G., 1893. On an intrusion of muscovite-biotite gneiss in the southeast Highlands
721 of Scotland and its accompanying metamorphism. *Quarterly Journal of the*
722 *Geological Society of London* **19**, 330-358.
- 723 Baxter, E. F., Ague, J. J., Depaolo, D. J., 2002. Prograde temperature-time evolution in
724 the Barrovian type-locality constrained by Sm/Nd garnet ages from Glen Clova,
725 Scotland. *Journal of the Geological Society* **159**, 71-82.
- 726 Bowring, S., Myrow, P., Landing, E., Ramezani, J., Grotzinger, J., 2003.
727 Geochronological constraints on terminal Neoproterozoic events and the rise of
728 metazoans: Geophysical Research Abstracts. **5**, p.13219.
- 729 Bowring, S. A., Grotzinger, J. P., Condon, D. J., Ramezani, J., Newall, M. J., Allen, P.
730 A., 2007. Geochronologic constraints on the chronostratigraphic framework of the
731 Neoproterozoic Huqf Supergroup, Sultanate of Oman. *Am J Sci* **307**, 1097-1145.
- 732 Brasier, M. D., Shields, G., 2000. Neoproterozoic chemostratigraphy and correlation of
733 the Port Askaig glaciation, Dalradian Supergroup of Scotland. *Journal of the*
734 *Geological Society* **157**, 909-914.
- 735 British Geological Survey, 2005. Aberfoyle. Scotland Sheet 38E. Bedrock and
736 Superficial geology. 1:50 000. Geology Series. British Geological Survey,
737 Keyworth, Nottingham
- 738 Brindley, G.W., 1982. Chemical compositions of berthierines, a review. *Clays and Clay*
739 *Minerals*, **30**, 153-155.

- 740 Canfield, D.E., Teske, A., 1996. Late Proterozoic rise in atmospheric oxygen
741 concentration inferred from phylogenetic and sulphur-isotope studies. *Nature* **382**,
742 127-132.
- 743 Canfield, D.E., Poulton, S.W., Narbonne, G.M., 2007. Late-Neoproterozoic Deep-Ocean
744 Oxygenation and the Rise of Animal Life. *Science* **315**, 92-95.
- 745 Canfield, D. E., Poulton, S. W., Knoll, A. H., Narbonne, G. M., Ross, G., Goldberg, T.,
746 Strauss, H., 2008. Ferruginous Conditions Dominated Later Neoproterozoic
747 Deep-Water Chemistry. *Science* **321**, 949-952.
- 748 Cawood, P. A., Nemchin, A. A., Smith, M., Loewy, S., 2003. Source of the Dalradian
749 Supergroup constrained by U-Pb dating of detrital zircon and implications for the
750 East Laurentian margin. *Journal of the Geological Society* **160**, 231-246.
- 751 Cawood, P. A., Nemchin, A. A., Strachan, R., Prave, T., Krabbendam, M., 2007.
752 Sedimentary basin and detrital zircon record along East Laurentia and Baltica
753 during assembly and breakup of Rodinia. *Journal of the Geological Society* **164**,
754 257-275.
- 755 Cawood, P. A., Nemchin, A. A., Strachan, R. A., Kinny, P. D., Loewy, S., 2004.
756 Laurentian provenance and an intracratonic tectonic setting for the Moine
757 Supergroup, Scotland, constrained by detrital zircons from the Loch Eil and Glen
758 Urquhart successions. *Journal of the Geological Society* **161**, 861-874.
- 759 Chew, D. M., Fallon, N., Kennelly, C., Crowley, Q., Pointon, M., 2010. Basic volcanism
760 contemporaneous with the Sturtian glacial episode in NE Scotland. *T Roy Soc*
761 *Edin-Earth*.
- 762 Cohen, A. S., Coe, A. L., Bartlett, J. M., Hawkesworth, C. J., 1999. Precise Re-Os ages of
763 organic-rich mudrocks and the Os isotope composition of Jurassic seawater. *Earth*
764 *and Planetary Science Letters* **167**, 159-173.
- 765 Condon, D. J., Prave, A. R., 2000. Two from Donegal: Neoproterozoic glacial episodes
766 on the northeast margin of Laurentia. *Geology* **28**, 951-954.
- 767 Condon, D., Zhu, M., Bowring, S., Wang, W., Yang, A., Jin, Y., 2005. U-Pb Ages from
768 the Neoproterozoic Doushantuo Formation, China. *Science*, **308**, 95-98.
- 769 Conliffe, J., Selby, D., Porter, S. J., Feely, M., 2010. Re-Os molybdenite dates from the
770 Ballachulish and Kilmelford Igneous Complexes (Scottish Highlands): age
771 constraints for late Caledonian magmatism. *Journal of the Geological Society*
772 **167**, 297-302.
- 773 Corsetti, F. A., Lorentz, N. J., 2006. On Neoproterozoic Cap Carbonates as
774 Chronostratigraphic Markers. In: Xiao, S., Kaufman, A. J., (Eds.), Neoproterozoic
775 Geobiology and Paleobiology. Springer, New York, pp. 273-294.
- 776 Creaser, R. A., Sannigrahi, P., Chacko, T., Selby, D., 2002. Further evaluation of the Re-
777 Os geochronometer in organic-rich sedimentary rocks: A test of hydrocarbon
778 maturation effects in the Exshaw Formation, Western Canada Sedimentary Basin.
779 *Geochimica et Cosmochimica Acta* **66**, 3441-3452.
- 780 Dalziel, I. W. D., 1994. Precambrian Scotland as a Laurentia-Gondwana Link - Origin
781 and Significance of Cratonic Promontories. *Geology* **22**, 589-592.
- 782 Dalziel, I. W. D., Soper, N. J., 2001. Neoproterozoic Extension on the Scottish
783 Promontory of Laurentia: Paleogeographic and Tectonic Implications. *The*
784 *Journal of Geology* **109**, 299-317.
- 785 Dempster, T. J., 1992. Zoning and recrystallization of phengitic micas: implications for
786 metamorphic equilibration. *Contrib. Mineral Petr.* **109**, 526-537.

- 787 Dempster, T.J., Rogers, G., Tanner, P.W.G., Bluck, B.J., Muir, R.J., Redwood, S.D.,
788 Ireland, T. R., Paterson, B. A., 2002. Timing of deposition, orogenesis and
789 glaciation within the Dalradian rocks of Scotland: constraints from U-Pb zircon
790 ages. *Journal of the Geological Society* **159**, 83-94.
- 791 Dewey, J., Mange, M., 1999. Petrography of Ordovician and Silurian sediments in the
792 western Irish Caledonides: tracers of a short-lived Ordovician continent-arc
793 collision orogeny and the evolution of the Laurentian Appalachian-Caledonian
794 margin. *Geological Society, London, Special Publications* **164**, 55-107.
- 795 Esser, B. K., Turekian, K. K., 1993. The osmium isotopic composition of the continental
796 crust. *Geochimica Cosmochimica Acta* **57**, 3093-3104.
- 797 Evans, J.A., 1996. Dating the transition of smectite to illite in Palaeozoic mudrocks using
798 the Rb-Sr whole-rock technique. *Journal of the Geological Society*, **153**, 101-108.
- 799 Evans, D. A. D., 2000. Stratigraphic, geochronological, and paleomagnetic constraints
800 upon the Neoproterozoic climatic paradox. *Am J Sci* **300**, 347-433.
- 801 Eyles, C. H., 1988. Glacially-Influenced and Tidally-Influenced Shallow Marine
802 Sedimentation of the Late Precambrian Port Askaig Formation, Scotland.
803 *Palaeogeography Palaeoclimatology Palaeoecology* **68**, 1-25.
- 804 Fairchild, I. J. Hambrey, M. J., 1995. Vendian basin evolution in East Greenland and NE
805 Svalbard. *Precambrian Research* **73**, 217-233.
- 806 Fairchild, I. J., Kennedy, M. J., 2007. Neoproterozoic glaciation in the Earth System.
807 *Journal of the Geological Society* **164**, 895-921.
- 808 Fanning, C.M., Link, P.K., 2004. U-Pb SHRIMP ages of Neoproterozoic (Sturtian)
809 glaciogenic Pocatello Formation, southeastern Idaho. *Geology*, **32**, 881-884.
- 810 Fike, D. A., Grotzinger, J. P., Pratt, L. M., Summons, R. E., 2006. Oxidation of the
811 Ediacaran Ocean. *Nature* **444**, 744-747.
- 812 Fletcher, T. P., Rushton, A. W. A., 2007. The Cambrian Fauna of the Leny Limestone,
813 Perthshire, Scotland. *Earth Env. Sci. T. R. So.* **98**, 199-218.
- 814 Friedrich, A. M., Hodges, K. V., Bowring, S. A., Martin, M. W., 1999. Geochronological
815 constraints on the magmatic, metamorphic and thermal evolution of the
816 Connemara Caledonides, western Ireland. *Journal of the Geological Society* **156**,
817 1217-1230.
- 818 Frimmel, H. E., On the reliability of stable carbon isotopes for Neoproterozoic
819 chemostratigraphic correlation. *Precambrian Research* **182** 239-253.
- 820 Giddings, J. A., Wallace, M. W., 2009. Facies-dependent $\delta^{13}\text{C}$ variation from a
821 Cryogenian platform margin, South Australia: Evidence for stratified
822 Neoproterozoic oceans? *Palaeogeography, Palaeoclimatology, Palaeoecology*
823 **271**, 196-214.
- 824 Glover, B. W., Key, R. M., May, F., Clark. G. G, Phillips, E. R., Chacksfield, B. C.,
825 1995. A Neoproterozoic multi-phase rift sequence: the Grampian and Appin
826 groups of the southwestern Monadhliath Mountains of Scotland. *Journal of the*
827 *Geological Society*, **152**, 391-406.
- 828 Glover, B. W., McKie, T., 1996. A sequence stratigraphical approach to the
829 understanding of basin history in orogenic Neoproterozoic successions: an
830 example from the central Highlands of Scotland. *Geological Society, London,*
831 *Special Publications* **103**, 257-269.
- 832 Glover, B. W., Winchester, J. A., 1989. The Grampian Group: a major Late Proterozoic
833 clastic sequence in the Central Highlands of Scotland. *Journal of the Geological*
834 *Society* **146**, 85-96.

- 835 Gorokhov, I. M., Semikhatov, M. A., Mel'nikov, N. N., Turchenko, T. L., Konstantinova,
836 G. V., Kut'yavin, E. P., 2001. Rb-Sr geochronology of middle Riphean shales, the
837 Yusmastakh Formation of the Anabar Massif, northern Siberia. *Stratigr Geo*
838 *Correl+* **9**, 213-231.
- 839 Halliday, A. N., Graham, C. M., Aftalion, M., Dymoke, P., 1989. The Depositional Age
840 of the Dalradian Supergroup - U-Pb and Sm-Nd Isotopic Studies of the Tayvallich
841 Volcanics, Scotland. *Journal of the Geological Society* **146**, 3-6.
- 842 Halverson, G. P., Hoffman, P. F., Schrag, D. P., Maloof, A. C., Rice, A. H. N., 2005.
843 Toward a Neoproterozoic composite carbon-isotope record. *Geological Society of*
844 *America Bulletin* **117**, 1181-1207.
- 845 Halverson, G. P., Hurtgen, M. T., 2007. Ediacaran growth of the marine sulfate reservoir.
846 *Earth and Planetary Science Letters* **263**, 32-44.
- 847 Halverson, G.P., Dudás, F.Ö., Maloof, A.C., Bowring, S.A., 2007a. Evolution of the
848 $^{87}\text{Sr}/^{86}\text{Sr}$ composition of Neoproterozoic seawater. *Palaeogeography,*
849 *Palaeoclimatology, Palaeoecology* **256**, 103-129.
- 850 Halverson, G. P., Maloof, A. C., Schrag, D. P., Dudás, F. Ö., Hurtgen, M., 2007b.
851 Stratigraphy and geochemistry of a ca 800 Ma negative carbon isotope interval in
852 northeastern Svalbard. *Chemical Geology* **237**, 5-27.
- 853 Hambrey, M. J., 1983. Correlation of Late Proterozoic tillites in the North Atlantic region
854 and Europe. *Geological Magazine* **120**, 209-232.
- 855 Harris, A. L., Haselock, P.J., Kennedy, M.J., Mendum, J.R., Long, C.B., Winchester, J.A.
856 Tanner, P.W.G., 1994. The Dalradian Supergroup in Scotland and Ireland. In:
857 Gibbons, W., Harris, A.L. (Ed.), *A Revised correlation of Precambrian rocks in*
858 *the British Isles*. Geological Society, London.
- 859 Harte, B., Pattison, D.R.M., Heuss-Assbichler, S., Hoernes, S., Masch, L., Strong, D.F.,
860 1991. Evidence of fluid phase behaviour and controls in the intrusive complex and
861 its aureole. In: Voll, G., Topel, J., Pattison, D.R.M., Seifert, F. (Ed.), *Equilibrium*
862 *and Kinetics in Contact Metamorphism: the Ballachulish Igneous Complex and*
863 *its Thermal Aureole*. Springer Verlag, Heidelberg.
- 864 Hattori, Y., Suzuki, K., Honda, M., Shimizu, H., 2003. Re-Os isotope systematics of the
865 Taklimakan Desert sands, moraines and river sediments around the taklimakan
866 desert, and of Tibetan soils. *Geochimica Et Cosmochimica Acta* **67**, 1203-1213.
- 867 Highton, A.J., Hyslop, E.K., Noble, S.R., 1999. U-Pb zircon geochronology of
868 migmatization in the northern Central Highlands: evidence for pre-Caledonian
869 (Neoproterozoic) tectonometamorphism in the Grampian block, Scotland. *Journal*
870 *of the Geological Society* **156**, 1195-1204.
- 871 Hill, A. C., Walter, M. R., 2000. Mid-Neoproterozoic (~830-750 Ma) isotope stratigraphy
872 of Australia and global correlation. *Precambrian Research* **100**, 181-211.
- 873 Hoffman, P. F., 1991. Did the Breakout of Laurentia Turn Gondwanaland Inside-Out?
874 *Science* **252**, 1409-1412.
- 875 Hoffman, P. F., Kaufman, A. J., Halverson, G. P., Schrag, D. P., 1998. A Neoproterozoic
876 snowball earth. *Science* **281**, 1342-1346.
- 877 Hoffman, P. F., Schrag, D. P., 2002. The snowball Earth hypothesis: testing the limits of
878 global change. *Terra Nova* **14**, 129-155.
- 879 Hoffmann, K. H., Condon, D. J., Bowring, S. A., Crowley, J. L., 2004. U-Pb zircon date
880 from the Neoproterozoic Ghaub Formation, Namibia: Constraints on Marinoan
881 glaciation. *Geology* **32**, 817-820.

- 882 Hutton, D. H. W., Alsop, G. I., 2004. Evidence for a major Neoproterozoic orogenic
883 unconformity within the Dalradian Supergroup of NW Ireland. *Journal of the*
884 *Geological Society* **161**, 629-640.
- 885 Hyde, W. T., Crowley, T. J., Baum, S. K., Peltier, W. R., 2000. Neoproterozoic/snowball
886 Earth/simulations with a coupled climate/ice-sheet model. *Nature* **405**, 425-429.
- 887 Jacobsen, S.B., Kaufman, A.J., 1999. The Sr, C and O isotopic evolution of
888 Neoproterozoic seawater. *Chemical Geology* **161**, 37-57.
- 889 Jaffe, L. A., Peucker-Ehrenbrink, B., Petsch, S. T., 2002. Mobility of rhenium, platinum
890 group elements and organic carbon during black shale weathering. *Earth and*
891 *Planetary Science Letters* **198**, 339-353.
- 892 Jensen, S., Saylor, B. Z., Gehling, J. G., Germs, G. J. B., 2000. Complex trace fossils
893 from the terminal Proterozoic of Namibia. *Geology* **28**, 143-146.
- 894 Jiang, G., Kaufman, A. J., Christie-Blick, N., Zhang, S., Wu, H., 2007. Carbon isotope
895 variability across the Ediacaran Yangtze platform in South China: Implications
896 for a large surface-to-deep ocean [δ] ^{13}C gradient. *Earth and Planetary*
897 *Science Letters* **261**, 303-320.
- 898 Kendall, B., Creaser, R. A., Calver, C. R., Raub, T. D., Evans, D. A. D., 2009a.
899 Correlation of Sturtian diamictite successions in southern Australia and
900 northwestern Tasmania by Re-Os black shale geochronology and the ambiguity of
901 "Sturtian"-type diamictite-cap carbonate pairs as chronostratigraphic marker
902 horizons. *Precambrian Research* **172**, 301-310.
- 903 Kendall, B., Creaser, R. A., Selby, D., 2009b. ^{187}Re - ^{187}Os geochronology of Precambrian
904 organic-rich sedimentary rocks. *Geological Society, London, Special Publications*
905 **326**, 85-107.
- 906 Kendall, B., Creaser, R. A., Gordon, G. W., Anbar, A. D., 2009c. Re-Os and Mo isotope
907 systematics of black shales from the Middle Proterozoic Velkerri and
908 Wollogorang Formations, McArthur Basin, northern Australia. *Geochimica Et*
909 *Cosmochimica Acta* **73**, 2534-2558.
- 910 Kendall, B., Creaser, R. A., Selby, D., 2006. Re-Os geochronology of postglacial black
911 shales in Australia: Constraints on the timing of "Sturtian" glaciation. *Geology* **34**,
912 729-732.
- 913 Kendall, B. S., Creaser, R. A., Ross, G. M., Selby, D., 2004. Constraints on the timing of
914 Marinoan 'Snowball Earth' glaciation by ^{187}Re - ^{187}Os dating of a Neoproterozoic
915 post-glacial black shale in Western Canada. *Earth and Planetary Science Letters*
916 **222**, 729-740.
- 917 Kennedy, M. J., Runnegar, B., Prave, A. R., Hoffmann, K. H., Arthur, M. A., 1998. Two
918 or four Neoproterozoic glaciations? *Geology* **26**, 1059-1063.
- 919 Kilburn, C., Shackleton, R. M., Pitcher, W. S., 1965. The stratigraphy and origin of the
920 Port Askaig boulder bed series (Dalradian). *Geol J* **4**, 343-360.
- 921 Kirschvink, J. L., 1992. Late Proterozoic low-latitude global glaciation: the snow ball
922 earth. In: Schopf, J. W. a. K., C (Ed.), *The Proterozoic Biosphere*. Cambridge
923 University Press, Cambridge.
- 924 Knoll, A. H., 2003. The geological consequences of evolution. *Geobiology* **1**, 3-14.
- 925 Knoll, A. H., Javaux, E. J., Hewitt, D., Cohen, P., 2006. Eukaryotic organisms in
926 Proterozoic oceans. *Philosophical Transactions of the Royal Society B-Biological*
927 *Sciences* **361**, 1023-1038.
- 928 Levasseur, S., Birck, J., Allègre, C.J., 1999. The osmium riverine flux and oceanic mass
929 balance of osmium. *Earth and Planetary Science Letters*, **174**, 7-23.

- 930 Li, Z. X., Bogdanova, S. V., Collins, A. S., Davidson, A., De Waele, B., Ernst, R. E.,
 931 Fitzsimons, I. C. W., Fuck, R. A., Gladkochub, D. P., Jacobs, J., Karlstrom, K. E.,
 932 Lu, S., Natapov, L. M., Pease, V., Pisarevsky, S. A., Thrane, K., Vernikovsky, V.,
 933 2008. Assembly, configuration, and break-up history of Rodinia: A synthesis.
 934 *Precambrian Research* **160**, 179-210.
- 935 Li, Z.-X., Evans, D.A.D., 2010. Late Neoproterozoic 40° intraplate rotation within
 936 Australia allows for a tighter-fitting and longer-lasting Rodinia. *Geology*, **39**, 39-
 937 42.
- 938 Litherland, M., 1980. The Stratigraphy of the Dalradian Rocks around Loch Creran,
 939 Argyll. *Scottish Journal of Geology* **16**, 105-123.
- 940 Logan, G. A., Hayes, J. M., Hieshima, G. B., Summons, R. E., 1995. Terminal
 941 Proterozoic reorganization of biogeochemical cycles. *Nature* **376**, 53-56.
- 942 Logan, G. A., Summons, R. E., Hayes, J. M., 1997. An isotopic biogeochemical study of
 943 Neoproterozoic and Early Cambrian sediments from the Centralian Superbasin,
 944 Australia. *Geochimica Et Cosmochimica Acta* **61**, 5391-5409.
- 945 Ludwig, K., 2003. Isoplot/Ex, version 3: a geochronological toolkit for Microsoft Excel.
 946 *Geochronology Center Berkeley*.
- 947 Ludwig, K. R., 1980. Calculation of uncertainties of U-Pb isotope data. *Earth and*
 948 *Planetary Science Letters* **46**, 212-220.
- 949 Macdonald, F.A., Schmitz, M.D., Crowley, J.L., Roots, C.F., Jones, D.S., Maloof, A.C.,
 950 Strauss, J.V., Cohen, P.A., Johnston, D.T., Schrag, D.P., 2010a. Calibrating the
 951 Cryogenian. *Science* **327**, 1241-1243.
- 952 Macdonald, F. A., Cohen, P. A., Dudas, F. O., Schrag, D. P., 2010b. Early
 953 Neoproterozoic scale microfossils in the Lower Tindir Group of Alaska and the
 954 Yukon Territory. *Geology* **38**, 143-146.
- 955 Mao, J., Lehmann, B., Du, A., Zhang, G., Ma, D., Wang, Y., Zeng, M., Kerrich, R., 2002.
 956 Re-Os Dating of Polymetallic Ni-Mo-PGE-Au Mineralization in Lower Cambrian
 957 Black Shales of South China and its geological significance. *Economic Geology*
 958 **97**, 1051-1061.
- 959 Martin, M. W., Grahdankin, D. V., Bowring, S. A., Evans, D. A., D., Fedonkin, M. A.,
 960 Kirschvink, J. L., 2000. Age of Neoproterozoic Bilatarian Body and Trace Fossils,
 961 White Sea, Russia: Implications for Metazoan Evolution. *Science* **288**, 841-845.
- 962 McCay, G. A., Prave, A. R., Alsop, G. I., Fallick, A. E., 2006. Glacial trinity:
 963 Neoproterozoic Earth history within the British-Irish Caledonides. *Geology* **34**,
 964 909-912.
- 965 Meert, J. G., 2007. Testing the Neoproterozoic glacial models. *Gondwana Research* **11**,
 966 573-574.
- 967 Melezhik, V. A., Gorokhov, I. M., Kuznetsov, A. B., Fallick, A. E., 2001.
 968 Chemostratigraphy of Neoproterozoic carbonates: implications for 'blind dating'.
 969 *Terra Nova* **13**, 1-11.
- 970 Melezhik, V. A., Roberts, D., Fallick, A. E., Gorokhov, I. M., 2008. The Shuram-
 971 Wonoka event recorded in a high-grade metamorphic terrane: insight from the
 972 Scandinavian Caledonides. *Geological Magazine* **145**, 161-172.
- 973 Morton, J.P., Long, L.E., 1982. Rb-Sr Ages of Precambrian Sedimentary-Rocks in the
 974 USA. *Precambrian Research*, **18**, (1-2), 133-138.
- 975 Narbonne, G. M., Gehling, J. G., 2003. Life after snowball: The oldest complex
 976 Ediacaran fossils. *Geology* **31**, 27-30.

- 977 Neilson, J. C., Kokelaar, B. P., Crowley, Q. G., 2009. Timing, relations and cause of
978 plutonic and volcanic activity of the Siluro-Devonian post-collision magmatic
979 episode in the Grampian Terrane, Scotland. *Journal of the Geological Society*
980 **166**, 545-561.
- 981 Noble, S. R., Hyslop, E. K., Highton, A. J., 1996. High precision U-Pb monazite
982 geochronology of the c. 806 Ma Grampian Shear Zone and the implications for
983 the evolution of the Central Highlands of Scotland. *Journal of the Geological*
984 *Society*, **153**, 511-514.
- 985 Ogg, J. G., Ogg, G., Gradstein, F.M., 2008. *The Concise Geologic Time Scale*.
986 Cambridge University Press, Cambridge.
- 987 Ohr, M., Halliday, A.N., Peacor, D.R., 1991 Sr and Nd Isotopic Evidence for Punctuated
988 Clay Diagenesis, Texas Gulf-Coast. *Earth and Planetary Science Letters*, **105**,
989 110-126.
- 990 Oliver, G. J. H., 2001. Reconstruction of the Grampian episode in Scotland: its place in
991 the Caledonian Orogeny. *Tectonophysics* **332**, 23-49.
- 992 Pattison, D. R. M., 2006. The fate of graphite in prograde metamorphism of pelites: An
993 example from the Ballachulish aureole, Scotland. *Lithos* **88**, 85-99.
- 994 Pattison, D. R. M., Harte, B., 1997. The geology and evolution of the Ballachulish
995 Igneous Complex and Aureole. *Scot J Geol* **33**, 1-29.
- 996 Peucker-Ehrenbrink, B., Jahn, B.-m., 2001. Rhenium-osmium isotope systematics and
997 platinum group element concentrations: Loess and the upper continental crust.
998 *Geochem. Geophys. Geosyst.* **2**.
- 999 Piasecki, M. A. J., 1980. New light on the Moine rocks of the Central Highlands of
1000 Scotland. *Journal of the Geological Society* **137**, 41-59.
- 1001 Prave, A. R., 1999. The Neoproterozoic Dalradian Supergroup of Scotland: an alternative
1002 hypothesis. *Geological Magazine* **136**, 609-617.
- 1003 Prave, A. R., Fallick, A. E., Thomas, C. W., Graham, C. M., 2009a. A composite C-
1004 isotope profile for the Neoproterozoic Dalradian Supergroup of Scotland and
1005 Ireland. *Journal of the Geological Society* **166**, 845-857.
- 1006 Prave, A. R., Strachan, R. A., Fallick, A. E., 2009b. Global C cycle perturbations
1007 recorded in marbles: a record of Neoproterozoic Earth history within the
1008 Dalradian succession of the Shetland Islands, Scotland. *Journal of the Geological*
1009 *Society* **166**, 129-135.
- 1010 Preiss, W. V., 2000. The Adelaide Geosyncline of South Australia and its significance in
1011 Neoproterozoic continental reconstruction. *Precambrian Research* **100**, 21-63.
- 1012 Pringle, J., 1939. The discovery of Cambrian trilobites in the Highland Border rocks near
1013 Callander, Perthshire. *Report of the British Association for the Advancement of*
1014 *Science* **252**.
- 1015 Rainbird, R.H., Hamilton, M.A., Young, G.M., 2001. Detrital zircon geochronology and
1016 provenance of the Torridonian, NW, Scotland: *Journal of the Geological Society*,
1017 **158**, 15-27
- 1018 Ravizza, G., Turekian, K. K., 1989. Application of the ^{187}Re - ^{187}Os system to black shale
1019 geochronometry. *Geochimica et Cosmochimica Acta* **53**, 3257-3262.
- 1020 Ravizza, G., Turekian, K.K., Hay, B.J., 1991. The geochemistry of rhenium and osmium
1021 in recent sediments from the Black Sea. *Geochim. Cosmochim. Acta.* **55**, 3741-
1022 3752.

- 1023 Rogers, G., Dunning, G. R., 1991. Geochronology of appinitic and related granitic
1024 magmatism in the W Highlands of Scotland: constraints on the timing of
1025 transcurrent fault movement. *Journal of the Geological Society* **148**, 17-27.
- 1026 Rooney, A. D., Selby, D., Houzay, J.-P., Renne, P. R., 2010. Re-Os geochronology of a
1027 Mesoproterozoic sedimentary succession, Taoudeni basin, Mauritania:
1028 Implications for basin-wide correlations and Re-Os organic-rich sediments
1029 systematics. *Earth and Planetary Science Letters* **289**, 486-496.
- 1030 Sawaki, Y., Kawai, T., Shibuya, T., Tahata, M., Omori, S., Komiya, T., Yoshida, N.,
1031 Hirata, T., Ohno, T., Windley, B. F., Maruyama, S., 2010. $^{87}\text{Sr}/^{86}\text{Sr}$
1032 chemostratigraphy of Neoproterozoic Dalradian carbonates below the Port Askaig
1033 Glaciogenic Formation, Scotland. *Precambrian Research* **179**, 150-164.
- 1034 Scott, C., Lyons, T.W., Bekker, A., Shen, Y., Poulton, S.W., Chu, X., Anbar, A.D., 2008.
1035 Tracing the stepwise oxygenation of the Proterozoic ocean. *Nature*, **452**, 456-460.
- 1036 Selby, D., 2007. Direct Rhenium-Osmium age of the Oxfordian-Kimmeridgian boundary,
1037 Staffin bay, Isle of Skye, U.K., and the Late Jurassic time scale. *Norwegian*
1038 *Journal of Geology*. **87**, 9.
- 1039 Selby, D., 2009. U-Pb zircon geochronology of the Aptian / Albian boundary implies that
1040 the GL-O international glauconite standard is anomalously young. *Cretaceous*
1041 *Research*, **30**, 1263-1267.
- 1042 Selby, D., Creaser, R. A., 2003. Re-Os geochronology of organic rich sediments: an
1043 evaluation of organic matter analysis methods. *Chemical Geology* **200**, 225-240.
- 1044 Selby, D., Creaser, R. A., 2005. Direct radiometric dating of the Devonian-Mississippian
1045 time-scale boundary using the Re-Os black shale geochronometer. *Geology* **33**,
1046 545-548.
- 1047 Selby, D., Creaser, R. A., Stein, H. J., Markey, R. J., Hannah, J. L., 2007. Assessment of
1048 the Re^{-187} decay constant by cross calibration of Re-Os molybdenite and U-Pb
1049 zircon chronometers in magmatic ore systems. *Geochimica Et Cosmochimica*
1050 *Acta* **71**, 1999-2013.
- 1051 Selby, D., Mutterlose, J., Condon, D.J., 2009. U-Pb and Re-Os geochronology of the
1052 Aptian / Albian and Cenomanian / Turonian stage boundaries and Re-Os
1053 systematics in organic-rich sediments. *Chemical Geology*, **265**, 394-409.
- 1054 Slack, J.F., Jiang, W.T., Peacor, D.R., Okita, P.M., 1992. Hydrothermal and metamorphic
1055 berthierine from the Kidd Creek Volcanogenic Massive Sulfide Deposit,
1056 Timmins, Ontario. *Canadian Mineralogist*. **30**, 1127-1142.
- 1057 Smith, M., Robertson, S., Rollin, K. E., 1999. Rift basin architecture and stratigraphical
1058 implications for basement-cover relationships in the Neoproterozoic Grampian
1059 Group of the Scottish Caledonides. *Journal of the Geological Society* **156**, 1163-
1060 1173.
- 1061 Smoliar, M. I., Walker, R. J., Morgan, J. W., 1996. Re-Os isotope constraints on the age
1062 of Group IIA, IIIA, IVA, and IVB iron meteorites. *Science* **271**, 1099-1102.
- 1063 Soper, N. J., 1994. Was Scotland a Vendian RRR junction? *Journal of the Geological*
1064 *Society* **151**, 579-582.
- 1065 Soper, N. J., England, R. W., 1995. Vendian and Riphean rifting in NW Scotland.
1066 *Journal of the Geological Society* **152**, 11-14.
- 1067 Soper, N. J., Ryan, P. D., Dewey, J. F., 1999. Age of the Grampian orogeny in Scotland
1068 and Ireland. *Journal of the Geological Society* **156**, 1231-1236.
- 1069 Spencer, A. M., 1971. Late Precambrian glaciation in Scotland. *Memoirs of the*
1070 *Geological Society of London* **6**, 1-100.

- 1071 Strachan, R. A., Smith, M., Harris, A.L., Fettes, D.J., 2002. The Northern Highland and
 1072 Grampian terranes. In: Trewhin, N. H. (Ed.), *The Geology of Scotland*. The
 1073 Geological Society, London.
- 1074 Sun, W., Arculus, R. J., Bennett, V. C., Eggins, S. M., Binns, R. A., 2003. Evidence for
 1075 rhenium enrichment in the mantle wedge from submarine arc-like volcanic
 1076 glasses (Papua New Guinea). *Geology* **31**, 845-848.
- 1077 Tanner, P. W. G., Alsop, G. I., Hutton, D. H. W., 2005. Discussion on evidence for a
 1078 major Neoproterozoic orogenic unconformity within the Dalradian Supergroup of
 1079 NW Ireland. *Journal of the Geological Society* **162**, 221-224.
- 1080 Tanner, P. W. G., Evans, J. A., 2003. Late Precambrian U-Pb titanite age for peak
 1081 regional metamorphism and deformation (Knoydartian orogeny) in the western
 1082 Moine, Scotland. *Journal of the Geological Society* **160**, 555-564.
- 1083 Tanner, P. W. G., Pringle, M. S., 1999. Testing for the presence of a terrane boundary
 1084 within Neoproterozoic (Dalradian) to Cambrian siliceous turbidites at Callander,
 1085 Perthshire, Scotland. *Journal of the Geological Society* **156**, 1205-1216.
- 1086 Tanner, P. W. G., Sutherland, S., 2007. The Highland Border Complex, Scotland: a
 1087 paradox resolved. *Journal of the Geological Society* **164**, 111-116.
- 1088 Thomas, C., Graham, C., Ellam, R., Fallick, A., 2004. $^{87}\text{Sr}/^{86}\text{Sr}$ chemostratigraphy of
 1089 Neoproterozoic Dalradian limestones of Scotland and Ireland: constraints on
 1090 depositional ages and time scales. *Journal of the Geological Society* **161**, 229-
 1091 242.
- 1092 Thomson, J., 1871. On the occurrence of pebbles and boulders of granite in schistose
 1093 rocks on Islay, Scotland *Report of the 40th Meeting of the British Association for*
 1094 *the Advancement of Science*, Liverpool.
- 1095 Thomson, J., 1877. On the geology of the island of Islay. *Transactions of the Geological*
 1096 *Society of Glasgow* **5**, 200-222.
- 1097 Tilley, C. E., 1925. A preliminary survey of metamorphic zones in the southern
 1098 Highlands of Scotland. *Quarterly Journal of the Geological Society of London* **81**.
- 1099 Trindade, R. I. F., Macouin, M., 2007. Palaeolatitude of glacial deposits and
 1100 palaeogeography of Neoproterozoic ice ages. *Comptes Rendus Geosciences* **339**,
 1101 200-211.
- 1102 Vidal, G., Moczydlowska-Vidal, M., 1997. Biodiversity, Speciation, and Extinction
 1103 Trends of Proterozoic and Cambrian Phytoplankton. *Paleobiology* **23**, 230-246.
- 1104 Voll, G., Topel, J., Pattison, D.R.M., Seifert, F., 1991. Equilibrium and Kinetics in
 1105 Contact Metamorphism: The Ballachulish Igneous Complex and its Aureole. .
 1106 Springer Verlag, Heidelberg.
- 1107 Walker, R. J., Horan, M. F., Morgan, J. W., Becker, H., Grossman, J. N., Rubin, A. E.,
 1108 2002a. Comparative ^{187}Re - ^{187}Os systematics of chondrites: Implications regarding
 1109 early solar system processes. *Geochimica Et Cosmochimica Acta* **66**, 4187-4201.
- 1110 Walker, R. J., Prichard, H. M., Ishiwatari, A., Pimentel, M., 2002b. The osmium isotopic
 1111 composition of convecting upper mantle deduced from ophiolite chromites.
 1112 *Geochimica Et Cosmochimica Acta* **66**, 329-345.
- 1113 Walsh, J. A., 2007. The use of the scanning electron microscope in the determination of
 1114 the mineral composition of Ballachulish slate. *Materials Characterization* **58**,
 1115 1095-1103.
- 1116 Yang, G., Hannah, J. L., Zimmerman, A., Stein, H. J., Bekker, A., 2009. Re-Os
 1117 depositional age for Archean carbonaceous slates from the southwestern Superior

1118 Province: Challenges and insights. *Earth and Planetary Science Letters* **280**, 83-
1119 92.
1120 Zhou, C., Tucker, R., Xiao, S., Peng, Z., Yuan, X., Chen, Z., 2004. New constraints on
1121 the ages of Neoproterozoic glaciations in south China. *Geology* **32**, 437-440.
1122

1123

1124 **Figure Captions**

1125 Figure 1: Simplified geological and location map highlighting the fourfold division of the
1126 Dalradian Supergroup of the Grampian Terrane (modified from Harris et al., 1994;
1127 Thomas et al., 2004). Abbreviations of sampling locations: BA – Ballachulish Slate
1128 quarry; LQ - Leny Limestone quarry.

1129

1130 Figure 2: Generalised stratigraphic column of the Dalradian Supergroup with glaciogenic
1131 horizons and the purported Bitter Springs anomaly suggested by Prave et al., (2009) but
1132 refuted by the new Re-Os geochronology data. See text for details. BA – Ballachulish
1133 Slate Formation; LQ – Leny Limestone Formation. (1. Halliday et al., 1989; 2. Dempster
1134 et al., 2002; 3. This study; 4. Noble et al., 1996). Modified from Prave et al. (2009a).

1135

1136 Figure 3: Re-Os isochron diagram for the Ballachulish Slate Formation using various
1137 digestion mediums a) the $\text{CrO}_3\text{-H}_2\text{SO}_4$ digestion method, b) inverse *aqua-regia* digestion,
1138 c) both digestion analyses ($\text{CrO}_3\text{-H}_2\text{SO}_4$ solid line, inverse *aqua-regia* dashed line). Inset
1139 diagrams show the deviation of each point from the $\text{CrO}_3\text{-H}_2\text{SO}_4$ best-fit regression. A
1140 Model 1 isochron is accomplished by assuming scatter along the regression line is
1141 derived only from the input 2σ uncertainties for $^{187}\text{Re}/^{188}\text{Os}$ and $^{187}\text{Os}/^{188}\text{Os}$, and ρ (rho).

1142

1143 Figure 4: Re-Os isochron diagram for the Leny Slate Member. The dashed line represents
1144 a 512 Ma reference line with the Os_i value of 0.8 representing Cambrian seawater (Mao
1145 et al., 2002; Jiang et al., 2003). The 512 Ma age assigned for the Leny Limestone is based
1146 on a trilobite fauna (Fletcher and Rushton, 2007). See text for discussion.

1147

1148 Figure 5: Graphic illustration of Re-Os geochronology data and Os_i values for
1149 Cryogenian and Sturtian (*sensu stricto*) pre and post glacial horizons. See text for
1150 discussion. Data from 1 = Ballachulish Slate Formation (this study); 2 = Aralka

1151 Formation (Kendall et al., 2006); 3 = Tapley Hill Formation (Kendall et al., 2006); 4 =
1152 Black River Dolomite (Kendall et al., 2009a)

1153

1154 **Tables**

1155 Table 1: Re-Os isotope data for the Ballachulish Slate and Leny Slate samples.

Accepted Manuscript

1 **Re-Os geochronology of the Neoproterozoic – Cambrian Dalradian**
2 **Supergroup of Scotland and Ireland: Implications for Neoproterozoic**
3 **stratigraphy, glaciations and Re-Os systematics**

4

5 Alan D. Rooney^{1*}, David M. Chew², David Selby¹

6 ¹Department of Earth Sciences, University of Durham, DH1 3LE, UK

7 ²Department of Geology, Trinity College Dublin, Dublin 2, Ireland

8 * Corresponding author: Tel. +44 0191 334 2300; Fax. +44 0191 334 2301.

9 *E-mail address:* alan.rooney@durham.ac.uk (A.D. Rooney).

10

11 **Abstract**

12 New Re-Os geochronology for the Ballachulish Slate Formation of the Dalradian
13 Supergroup, Scotland yields a depositional age of 659.6 ± 9.6 Ma. This age represents the
14 first successful application of the Re-Os system to rocks that have extremely low Re and
15 Os abundances (<1 ppb and <50 ppt, respectively). The Re-Os age represents a maximum
16 age for the glaciogenic Port Askaig Formation and refutes previous chemostratigraphic
17 and lithostratigraphic studies which correlated the Port Askaig Formation with a series of
18 middle Cryogenian (ca. 715 Ma) glacials. Additionally, the Re-Os age strongly suggests
19 that the Port Askaig Formation may be correlative with the ~ 650 Ma end-Sturtian
20 glaciations of Australia. As a consequence, the correlation of the Ballachulish Limestone
21 Formation with the ca. 800 Ma Bitter Springs anomaly is not tenable. Initial Os isotope
22 data from the Ballachulish Slate Formation coupled with data from Australia reveals a
23 radiogenic $^{187}\text{Os}/^{188}\text{Os}$ isotope composition (~ 0.8 to 1.0) for seawater during the
24 Neoproterozoic, which is similar to that of modern seawater (1.06).

25 We also report a young, highly imprecise Re-Os age (310 ± 110 Ma) for the Early
26 Cambrian Leny Limestone Formation which is constrained biostratigraphically by a
27 polymerid and miomerid trilobite fauna. We suggest, based on the mineralogy of the
28 Leny Limestone, (kaolinite, muscovite and a serpentine group mineral, berthierine), that
29 the Re-Os systematics have been disturbed by post-depositional fluid flow associated
30 with Palaeozoic igneous intrusions. However, it is evident from the Ballachulish Slate
31 Formation results that anhydrous metamorphism does not disturb the Re-Os
32 geochronometer.

33

34 **Keywords:** Re-Os, Dalradian, Neoproterozoic, Sturtian, Rodinia, Laurentia

Accepted Manuscript

35 1. Introduction

36 Neoproterozoic strata record a number of significant events such as the transition
37 from stratified Proterozoic oceans with oxic surface waters and anoxic deep waters to a
38 [more-or-less fully oxygenated ocean](#) (Anbar and Knoll, 2002; Knoll, 2003; Fike et al.,
39 [2006](#); Halverson and Hurtgen, 2007; Canfield et al., 2008). Major changes in biological
40 systems and evolutionary developments occurred towards the end of the Proterozoic
41 including the [evolution of metazoans](#) (Logan et al., 1995; 1997; Vidal and
42 Moczydlowska-Vidal, 1997; Jensen et al., 2000; Martin et al., 2000; Narbonne and
43 Gehling, 2003; Knoll et al., 2006; Macdonald, 2010a, b). Additionally, the
44 Neoproterozoic was a time of major climatic fluctuation with a number of extreme glacial
45 events recorded in the rock record (e.g. the “Snowball Earth” of Kirschvink, 1992;
46 Hoffman et al., 1998; Hoffman and Schrag, 2002 or the “Slushball Earth” of Hyde et al.,
47 2000). However, there is at present, no consensus as to the cause, extent, duration or
48 number of these glacial events (Kennedy et al., 1998; Evans, 2000; Fairchild and
49 Kennedy, 2007). The lack of precise [and accurate](#) geochronological data has severely
50 hindered attempts to develop a chronological framework for the Neoproterozoic. In
51 particular, understanding and constraining the extent and duration of these glacial events
52 has relied upon lithostratigraphy and chemostratigraphy with only a few glaciogenic
53 successions constrained by robust geochronological data ([Hoffmann et al., 2004](#); [Zhou et](#)
54 [al., 2004](#); [Kendall et al., 2004](#); [2006](#); [2009a](#); [Condon et al., 2005](#); [Bowring et al., 2007](#);
55 [Macdonald et al., 2010a](#)).

56 During the Neoproterozoic, the continental masses of Laurentia, Baltica and
57 Amazonia were juxtaposed as a result of various orogenic events to form the
58 supercontinent Rodinia (e.g. Li et al., 2008 and references therein). During the break-up
59 of Rodinia which commenced [at ca. 750 Ma](#) there was a period of intracontinental
60 extension and basin genesis along the eastern margin of Laurentia (Harris et al., 1994;
61 Soper, 1994; Cawood et al., 2007). Scotland occupied a unique position within the
62 Rodinia supercontinent lying close to the junction of the Laurentian, Baltica and
63 Amazonian continental blocks (Dalziel, 1994). The sedimentary basins that formed
64 during the formation and breakup of Rodinia are preserved in Scotland as the
65 Torridonian, Moine and Dalradian Supergroups (Anderton, 1982; 1985; Rainbird et al.,
66 2001; Strachan et al., 2002; Cawood et al., 2003; 2004; 2007).

67 The Dalradian Supergroup of Scotland and Ireland is a metasedimentary
68 succession that was deposited on the eastern margin of Laurentia during the late
69 Neoproterozoic and Early Cambrian. Existing constraints imply the base is younger than
70 800 Ma and it extends to at least 510 Ma (Harris et al., 1994; Smith et al., 1999; Prave et
71 al., 2009a). Despite its importance in regional and global studies of the Proterozoic, our
72 understanding of the Dalradian sequence suffers from a lack of radiometric ages
73 (Halliday et al., 1989; Dempster et al., 2002). In an attempt to improve the
74 chronostratigraphy of the Dalradian, several workers have applied lithostratigraphic and
75 chemostratigraphic tools with varying levels of success (Prave, 1999; Brasier and Shields,
76 2000; Condon and Prave, 2000; Thomas et al., 2004; McCay et al., 2006; Prave et al.,
77 2009a; Sawaki et al., 2010). [These studies have improved our knowledge of the
78 Proterozoic ocean chemistry and the environmental conditions of deposition within the
79 Dalradian sedimentary basin. However, chemostratigraphic tools cannot provide absolute
80 ages and ultimately rely upon correlation with sequences which have robust radiometric
81 and / or biostratigraphic age constraints](#) (Melezhik et al., 2001; 2007; Fairchild and
82 Kennedy, 2007; Jiang et al., 2007; Meert, 2007; Giddings and Wallace, 2009; Frimmel,
83 2010). As a result, obtaining precise and accurate radiometric ages remain a priority for
84 resolving many of the issues regarding global correlations.

85 The rhenium-osmium (Re-Os) geochronometer has been shown to provide robust
86 depositional ages even for sedimentary rocks that have experienced hydrocarbon
87 maturation, greenschist metamorphism and flash pyrolysis associated with igneous
88 intrusions (Creaser et al., 2002; Kendall et al., 2004; 2006; 2009a, b; Selby and Creaser,
89 2005; Rooney et al., 2010). Thus, the Re-Os system represents an accurate, precise and
90 reliable geochronometer for providing depositional age data for the Dalradian
91 metasediments and constructing a chronostratigraphic framework for the
92 chemostratigraphic, tectonostratigraphic and lithostratigraphic datasets.

93 Here, we present new Re-Os age that constrain the depositional age of a
94 sedimentary unit from the Dalradian Supergroup. The Re-Os data also provides an
95 estimate for the osmium isotope composition of seawater in the Dalradian basin during
96 the Neoproterozoic and ultimately provide a maximum depositional age for a key
97 Neoproterozoic glacial horizon. A further aspect of this study involves the application of
98 Re-Os geochronology to sedimentary units with low Re and Os abundances (<1 ppb Re

99 and <50 ppt Os) to provide accurate and precise geochronology. Additionally, this work
100 presents results from a sedimentary unit (Leny Limestone Formation) in which the Re-Os
101 geochronometer has been disturbed as a result of post-depositional fluid flow. The results
102 from this study provide us with new insights into the robustness of the Re-Os
103 geochronometer.

104

105 **2. Geological Setting**

106 *2.1. The Dalradian Supergroup*

107 The Dalradian Supergroup of Scotland and Ireland consists of a thick (~25 km)
108 metasedimentary succession and a minor amount of mafic volcanics deposited on the
109 eastern margin of the Laurentian craton during the [Neoproterozoic to Early Cambrian](#)
110 (Fig. 1; Harris et al., 1994 and references therein). This quoted thickness of the Dalradian
111 Supergroup is a cumulative thickness from all subgroups and is not a true reflection of
112 sediment thickness. Many aspects of basin genesis have proved controversial, with little
113 consensus apparent even after more than a century of studies. Most models for Dalradian
114 deposition invoke a long, shallow-marine, ensialic basin which underwent prolonged
115 extension during the late Neoproterozoic, resulting in the eventual separation of Laurentia
116 from western Gondwana at ca. 550 Ma (Hoffman, 1991; Soper, 1994; Dalziel and Soper,
117 2001). An alternative model proposes that the lower portions of the Dalradian represented
118 a rapidly formed foredeep basin associated with the mid-Neoproterozoic (840 – 730 Ma)
119 Knoydartian Orogeny (Prave, 1999). In both models extensional tectonics played a major
120 role in the genesis of the upper portions of the Dalradian basin during the latest
121 Neoproterozoic to Early Cambrian.

122 Lithostratigraphic correlation of the Dalradian Supergroup is hampered by the
123 paucity of volcanic horizons suitable for U-Pb geochronology and the lack of
124 biostratigraphically diagnostic fossils (Fig. 2). Additionally, many portions of the
125 Dalradian sequence exhibit extreme facies variability along strike having experienced
126 complex polyphase deformation and metamorphism (Harris et al., 1994, Strachan et al.,
127 2002 and references therein). Despite these issues, a coherent lithostratigraphy has been
128 established from western Ireland to the Shetland Islands, 200 km north of mainland
129 Scotland (Harris et al., 1994).

130 The Dalradian Supergroup consists of four groups which are from oldest to
131 youngest; the Grampian, Appin, Argyll and Southern Highland groups (Figs. 1 and 2).

132 The basal Grampian Group crops out primarily in the Central Highlands although
133 possible correlatives exist on the north Grampian coast and on the Shetland Islands
134 (Strachan et al., 2002). The Grampian Group consists of up to 7 km of predominantly
135 marine, quartzo-feldspathic psammites and semi-pelites (Glover and Winchester, 1989;
136 Harris et al., 1994). The Grampian Group sedimentary succession displays sharp lateral
137 variations typical of a syn-rift origin (Soper and England, 1995; Banks et al., 2007). The
138 overlying Appin Group is exposed in a broad zone throughout Scotland and Ireland as far
139 north as the Shetland Islands. The Appin Group consists of up to 4 km of quartzite, semi-
140 pelites and phyllites deposited as a post-rift, thermal subsidence sequence (Litherland,
141 1980; Glover et al., 1995; Soper and England, 1995; Glover and McKie, 1996). The
142 overlying Argyll Group records rapid deepening of the basin following the shallow
143 marine conditions of the Appin Group (Anderton, 1985). The Argyll Group consists of a
144 thick heterogeneous succession of shelf sediments up to 9 km thick which passes upwards
145 into deep water turbidite and basinal facies and associated mafic volcanics (Anderton,
146 1982). The marked change from a shelf setting to deep water sedimentation is widely
147 ascribed to the onset of syn-depositional rifting. The basal subgroup (Islay Subgroup) of
148 the Argyll Group is marked by a distinctive and persistent tillite horizon; the Port Askaig
149 Formation, correlatives of which are traceable from Connemara in western Ireland to
150 Banffshire in NE Scotland (Anderton, 1985; Harris et al., 1994). The Southern Highland
151 Group (along with the newly defined Trossachs Group of Tanner and Sutherland, 2007)
152 marks the top of the Dalradian succession and consists of ca. 4 km of coarse-grained
153 turbiditic clastics and volcanoclastic strata (Anderton, 1985; Soper and England, 1995).
154 The Southern Highland Group is considered to represent the change from a period of
155 continental rifting and rupture to that of a thermally subsiding margin (Anderton, 1985).

156

157 *2.1.1. Glaciogenic horizons within the Dalradian and possible global* 158 *correlations*

159 The Port Askaig Formation of the Argyll Group is a thick (~900 m) succession of
160 diamictites interbedded with sandstone, conglomerate and mudstone (Kilburn et al., 1965;
161 Spencer, 1971; Eyles, 1988; Arnaud and Eyles, 2002). The formation represents the most

162 persistent and distinctive glaciogenic horizon within the Dalradian Supergroup (Fig. 2). A
163 glaciogenic origin was first recognised in the late nineteenth century (Thomson, 1871;
164 1877), and is described in detail in the classic memoir of Spencer (1971). The most
165 extensive outcrops of the Port Askaig Formation consists of ~400 m of coarse-grained
166 and poorly sorted diamictite interbedded with sandstone, mudstone and conglomerate
167 with some megaclasts in the diamictite exceeding 100 m in size (Spencer, 1971; Arnaud,
168 2004). Recent studies identified enriched $\delta^{13}\text{C}$ (+11.7‰) and unradiogenic $^{87}\text{Sr}/^{86}\text{Sr}$
169 (0.7067) in carbonate formations above and below the Port Askaig Formation (Brasier
170 and Shields, 2000; Sawaki et al., 2010). These data have been used to correlate the
171 glaciogenic horizon with the ca. 750 – 690 Ma global Sturtian glaciation (Brasier and
172 Shields, 2000; Fanning and Link, 2004; McCay et al., 2006; Macdonald et al., 2010a).
173 Two more stratigraphically limited glaciogenic units within the Dalradian Supergroup
174 have also been identified; the Stralinchy “Boulder Bed” Formation and the Inishowen -
175 Loch na Cille Ice Rafted Debris (IRD) Formations (Fig. 2; Condon and Prave, 2000;
176 McCay et al., 2006). The Stralinchy Formation occurs in the Easdale Subgroup in
177 Donegal in NW Ireland and has been correlated with the ~635 Ma global Marinoan
178 glaciation (Hoffmann et al., 2004; Condon et al., 2005; McCay et al., 2006). The Loch na
179 Cille and Inishowen glaciogenic formations occur within the uppermost Argyll Group
180 and basal Southern Highland Group respectively, and have been correlated with the 580
181 Ma Laurentian Gaskiers glacial event (Condon and Prave, 2000; Bowring et al., 2003).

182

183 2.2. Current chronological constraints for the Dalradian Supergroup

184 With the exception of *Bonnia-Ollenellus* Zone Early Cambrian trilobites and
185 inarticulate brachiopods of the upper Southern Highland Group, the Dalradian
186 Supergroup is almost entirely devoid of fossils (Pringle, 1939; Fletcher and Rushton,
187 2007). In addition, absolute chronological constraints on the age of Dalradian
188 sedimentation are also very sparse (Fig. 2). The oldest phase of volcanic activity in the
189 Dalradian Supergroup occurs within correlatives of the Port Askaig Formation in NE
190 Scotland (Chew et al., 2010). However, this thin tholeiitic pillow basalt has not been
191 dated thus far. The lower part of the Southern Highland Group in SW Scotland is
192 characterised by ca. 2 km of tholeiitic mafic volcanic rocks and sills (Tayvallich Volcanic
193 Formation). The Tayvallich Formation is cross cut by a 595 ± 4 Ma (U-Pb SHIRIMP)

194 keratophyre intrusion and a felsic tuff from this formation has yielded a U-Pb zircon age
195 of 601 ± 4 Ma (Halliday et al., 1989; Dempster et al., 2002). Pegmatites from the Central
196 Scottish Highlands has yielded a U-Pb monazite age of 806 ± 3 Ma although the
197 stratigraphic position of these pegmatites remains controversial (Noble et al., 1996).
198 These pegmatites have been suggested to intrude into Grampian Group rocks thus
199 providing a minimum age for these sediments (Noble et al., 1996; Highton et al., 1999).
200 However, other studies (e.g. Smith et al., 1999) propose that the pegmatites intrude into
201 the Dava and Glen Banchor successions which lie unconformably below the Grampian
202 Group and that therefore the Grampian Group is younger than 806 Ma (Smith et al.,
203 1999; Strachan et al., 2002).

204 Numerous studies have utilised $\delta^{13}\text{C}$, $\delta^{18}\text{O}$ and $^{87}\text{Sr}/^{86}\text{Sr}$ data from several different
205 carbonate units of the Dalradian Supergroup with the aim of correlation with global
206 chemostratigraphic curves (Brasier and Shields, 2000; Thomas et al., 2004; McCay et al.,
207 2006; Halverson et al., 2007a; Prave et al., 2009a; Sawaki et al., 2010). A composite $\delta^{13}\text{C}$
208 profile for the Dalradian Supergroup has been used to tentatively correlate the
209 Ballachulish Limestone of the Appin Group with the ca. 800 Ma Bitter Springs anomaly
210 (Prave et al., 2009a; Fig. 2). Additional correlations include the pre-Marinoan Trezona
211 anomaly and ca. 635 Ma Marinoan-equivalent cap carbonate sequence with units of the
212 middle Easdale Subgroup and the terminal Proterozoic (ca. 600 – 551 Ma) Shuram-
213 Wonoka anomaly in the Girlsta Limestone on Shetland (Melezhik et al., 2008; Prave et
214 al., 2009a, b).

215

216 *2.3. Metamorphism and deformation of the Dalradian Supergroup*

217 The Dalradian Supergroup of Scotland is one of the classic areas for the study of
218 regional and contact metamorphism (e.g., Barrow, 1893; Tilley, 1925; Baker, 1985; Voll
219 et al., 1991; Dempster et al., 1992; Pattison and Harte, 1997). The main phases of
220 regional metamorphism took place during the Grampian Orogeny. The Grampian
221 Orogeny is understood to be related to the collision of Laurentia with an oceanic arc
222 during the Early Ordovician and can be considered broadly equivalent to the Taconic
223 Orogeny of the Appalachians (Dewey and Mange, 1999; Soper et al., 1999).
224 Geochronological constraints for the Grampian Orogeny include U-Pb zircon ages from
225 syn-tectonic intrusives of 475 – 468 Ma and Sm-Nd metamorphic garnet crystallisation

226 ages of 473 – 465 Ma which date peak metamorphism (Friedrich et al., 1999; Baxter et
227 al., 2002).

228 The Dalradian sedimentary succession also experienced contact metamorphism
229 associated with the intrusion of numerous Late Caledonian (ca. 430 – 390 Ma; Oliver,
230 2001) granites throughout the Grampian Terrane of Scotland (Fig. 1). In addition to the
231 granites there are also a number of minor Late Palaeozoic intrusive suites recorded in the
232 Dalradian (Neilson et al., 2009 and references therein).

233

234 **3. Samples for this study**

235 Two localities were chosen for Re-Os geochronology analyses; the Ballachulish Slate
236 Formation from the Ballachulish Subgroup of the Appin Group and the Leny Limestone
237 Formation of the Southern Highland Group (Figs. 1 and 2). The Ballachulish Slate was
238 chosen to provide a maximum age constraint on the depositional age of the Port Askaig
239 Formation (Fig. 2). The Leny Limestone Formation was chosen as it contains the only
240 biostratigraphically diagnostic fauna found in the Dalradian Supergroup (Pringle, 1939;
241 Fletcher and Rushton, 2007). Additionally, the metasedimentary rocks of the Dalradian
242 Supergroup represent an opportunity to further our understanding of the effects of
243 regional and contact metamorphism on the Re-Os geochronometer.

244

245 *3.1. Appin Group – Ballachulish Slate Formation*

246 The Appin Group consists of three subgroups, the Lochaber, Ballachulish and Blair
247 Atholl (Fig. 2). The Ballachulish Slate Formation consists of ca. 400 m of pyritiferous
248 black slates and graphitic phyllites. Samples were collected on the eastern foreshore of
249 Loch Linnhe at the entrance to Loch Leven (56° 42. 1' N, 5° 11. 6' W; Fig. 1). In this
250 area, the top of the Ballachulish Slate Formation is estimated to be ca. 1 km below the
251 equivalent of the Port Askaig Formation (Litherland, 1980; Harris et al., 1994). Regional
252 metamorphic grade associated with the Grampian Orogeny varies from chlorite grade in
253 the NW to garnet grade in the SE. Estimates of P-T conditions range from ca. 450 - 550°
254 C from NW to SE, at ca. 6 kbar (Pattison and Voll, 1991). In addition to Grampian
255 regional metamorphism, the Ballachulish Slates also experienced Late Caledonian (ca.
256 430 Ma) igneous activity and contact metamorphism primarily associated with the well
257 characterised Ballachulish Igneous Complex (Pattison and Harte, 1997; Pattison, 2006).

258 The metamorphic aureole varies in width from ca. 400 to 1700 m, based upon the first
259 appearance of cordierite in metapelites (Pattison, 2006). Regional P-T conditions at the
260 time of intrusion are estimated at ca. 250 – 300° C at ca. 3 kbar. The age of the
261 Ballachulish Igneous Complex is constrained by Re-Os molybdenite and U-Pb zircon
262 ages of 433.5 ± 1.8 Ma and 428 ± 9.8 Ma, respectively (Conliffe et al., 2010; Rogers and
263 Dunning, 1991, recalculated by Neilson et al., 2009). Fluid flow between the intrusion
264 and the aureole was limited and there is no evidence for a large-scale hydrothermal
265 circulation system or associated mineralogical changes connected to the intrusion (Harte
266 et al., 1991; Pattison, 2006).

267 The slates analysed in this study were sampled ca. 2 km NNW of the NW contact of
268 the Ballachulish Igneous complex and are hence outside the aureole. The slates sampled
269 are black and massive with bedding occasionally still discernible and predominantly
270 orientated parallel to cleavage. X-ray diffractometry (XRD) studies indicate that the
271 Ballachulish Slates have a composition of quartz, mica, chlorite and feldspars (albite and
272 occasionally orthoclase), typical of an argillaceous slate. The samples of Ballachulish
273 slate used in this study are similar in composition to those described in greater detail by
274 Walsh (2007).

275

276 3.2. Southern Highland Group – Leny Limestone

277 The Leny Limestone forms part of the Keltie Water Grit Formation of the Southern
278 Highland Group. The formation consists of pale grey to white, siliceous grits, black
279 graphitic slates and rare locally fossiliferous limestones (Tanner and Pringle, 1999). The
280 limestones of this formation yield a fauna including polymerid and miomerid trilobites,
281 brachiopods, sponges, hyoliths and bradoriids (Fletcher and Rushton, 2007). The
282 miomerid trilobites indicate a stratigraphical age equivalent to the base of the paradoxidid
283 Amgan Stage of Siberia traditionally regarded as Middle Cambrian (511 – 506 Ma, Ogg
284 et al., 2008). However, the polymerid trilobites e.g., *Pagetides*, are forms from the
285 *Bonnia-Olenellus* Zone and are thus regarded as Lower Cambrian (516.5 – 512 Ma; Ogg
286 et al., 2008). An age of ca. 512 Ma has been adopted here as the age of the Leny
287 Limestone Formation (Fletcher and Rushton, 2007).

288 Black graphitic slates of the Leny Limestone Formation were sampled on the south-
289 easterly face of the Western Quarry (56° 15.5' N, 4° 13.1 W; Fig. 1). The metamorphic

290 grade during the Grampian Orogeny was low, with an estimated peak metamorphic
291 temperature of 270°C (Tanner and Pringle, 1999). Detrital biotite is preserved, albeit
292 commonly partially altered to chlorite. The locality is also the locus of several phases of
293 igneous activity such as intrusions of Devonian quartz-felsite dykes and Permo-
294 Carboniferous quartz dolerite dykes (British Geological Survey, 2005; Fletcher and
295 Rushton, 2007). The Devonian intrusion exhibits a 70 m fault offset, though this faulting
296 is not seen in the Permo-Carboniferous dyke suggesting faulting occurred prior to this
297 younger intrusive episode. XRD analysis of the Leny Limestone Formation slates reveal a
298 composition of quartz, micas (mainly muscovite), kaolinite and a serpentine-group
299 mineral with the chemical formula of $\text{Fe}_3\text{Si}_2\text{O}_5(\text{OH})_4$ suggested to represent berthierine
300 (Brindley, 1982).

301

302 4. Sampling and analytical methods

303 Sampling of the Ballachulish Slate and Leny Limestone Formations was limited
304 to a vertical interval of ca. 50 cm of stratigraphy across a lateral interval of several tens of
305 metres. Weathered material was removed from the outcrop prior to sampling of fresh
306 surfaces. Large (~100 g) samples were selected to ensure homogenisation of Re-Os
307 abundances in the samples (Kendall et al., 2009b). All samples were polished to remove
308 cutting and drilling marks to eliminate any potential contamination. The samples were
309 dried at 60 °C for ~12 hrs and then crushed to a fine powder of ~30 µm. The samples
310 were broken into chips with no metal contact and powdered in a ceramic dish using a
311 shatterbox.

312 Rhenium-osmium isotope analysis was carried out at Durham University's TOTAL
313 laboratory for source rock geochronology and geochemistry at the Northern Centre for
314 Isotopic and Elemental Tracing (NCIET). Sample digestion using a $\text{CrO}_3\text{-H}_2\text{SO}_4$ solution
315 is the preferred method for Re-Os geochronology as it has been shown to preferentially
316 liberate hydrogenous Re and Os, ultimately providing more precise ages (Selby and
317 Creaser, 2003; Kendall et al., 2004). An inverse *aqua-regia* solution was also employed
318 in an attempt to evaluate the contribution of detrital Re and Os in these samples. Previous
319 work has shown that *aqua-regia* digestion liberates both non-hydrogenous (detrital and
320 meteoritic) and hydrogenous Re and Os. This detrital Os component has been shown to
321 represent a source of geological scatter that results in determination of imprecise and / or

322 inaccurate depositional ages (Ravizza et al., 1991; Selby and Creaser, 2003; Kendall et
323 al., 2004).

324 Approximately 1 g of sample powder was digested together with a mixed tracer
325 (spike) solution of ^{190}Os and ^{185}Re in a $\text{Cr}^{\text{VI}}\text{-H}_2\text{SO}_4$ solution in a sealed carius tube at 220
326 $^\circ\text{C}$ for ~ 48 h (Selby and Creaser, 2003; Kendall et al., 2004). Through the use of the $\text{Cr}^{\text{VI}}\text{-}$
327 H_2SO_4 digestion media it is possible to preferentially liberate the hydrogenous Re and Os
328 components from the samples thus limiting any detrital component (Selby and Creaser,
329 2003; Kendall et al., 2004). For the inverse *aqua-regia* digestions approximately 1 g of
330 sample powder was dissolved together with a spike solution of ^{190}Os and ^{185}Re in a 1:2
331 acid mixture of 3 ml 12 N HCl and 6 ml of 16 N HNO_3 in a sealed carius tube at 220 $^\circ\text{C}$
332 for ~ 48 h (Selby and Creaser, 2003).

333 Rhenium and Os were purified from the acid solution using solvent extraction
334 (CHCl_3), micro-distillation and anion chromatography methods and analysed by negative
335 thermal ionisation mass spectrometry as outlined by Selby and Creaser (2003), and Selby
336 (2007). The purified Re and Os fractions were loaded onto Ni and Pt filaments,
337 respectively (Selby et al., 2007), with the isotopic measurements conducted using a
338 ThermoElectron TRITON mass spectrometer via static Faraday collection for Re and ion-
339 counting using a secondary electron multiplier in peak-hopping mode for Os. Average
340 procedural blanks for the $\text{Cr}^{\text{VI}}\text{-H}_2\text{SO}_4$ method during this study were 16.8 ± 0.06 pg and
341 0.43 ± 0.06 pg (1σ S.D., $n = 3$) for Re and Os respectively, with an average $^{187}\text{Os}/^{188}\text{Os}$
342 value of $\sim 0.25 \pm 0.11$ ($n = 3$). For the inverse *aqua-regia* method procedural blanks for
343 Re and Os were 1.9 ± 0.01 pg and 0.12 ± 0.06 pg, respectively (1σ S.D. $n = 2$) with an
344 average $^{187}\text{Os}/^{188}\text{Os}$ value of $\sim 0.4 \pm 0.5$ (1σ S.D., $n = 2$).

345 Uncertainties for $^{187}\text{Re}/^{188}\text{Os}$ and $^{187}\text{Os}/^{188}\text{Os}$ are determined by error propagation
346 of uncertainties in Re and Os mass spectrometer measurements, blank abundances and
347 isotopic compositions, spike calibrations and reproducibility of standard Re and Os
348 isotopic values using methods identical to previous studies (e.g., Kendall et al., 2004;
349 Selby and Creaser, 2005). The Re-Os isotopic data, 2σ calculated uncertainties for
350 $^{187}\text{Re}/^{188}\text{Os}$ and $^{187}\text{Os}/^{188}\text{Os}$ and the associated error correlation function (ρ) are
351 regressed to yield a Re-Os date using *Isoplot V. 3.0* with a λ ^{187}Re constant of $1.666 \times 10^{\text{-}}$
352 $^{11}\text{a}^{-1}$ (Ludwig, 1980; Smoliar et al., 1996; Ludwig, 2003).

353 To ensure and monitor long-term mass spectrometry reproducibility, in-house
354 standard solutions of Re and Os (Durham Romil Osmium Standard [DROsS]) are
355 repeatedly analysed at NCIET. The Re standard analysed during the course of this study
356 is made from 99.999% zone-refined Re ribbon and is considered to have an identical Re
357 isotopic composition to that of the AB-1 Re standard (Creaser et al., 2002; Selby and
358 Creaser, 2003; Kendall et al., 2004). The NCIET Re standard yields an average
359 $^{185}\text{Re}/^{187}\text{Re}$ ratio of 0.59772 ± 0.00172 (1 SD, $n = 114$). This is in excellent agreement
360 with the value reported for the AB-1 standard (Creaser et al., 2002). The Os isotope
361 reference material (DROsS) yields an $^{187}\text{Os}/^{188}\text{Os}$ ratio of 0.106093 ± 0.00015 (1 SD, $n =$
362 36). The isotopic compositions of these solutions are identical within uncertainty to those
363 reported by Rooney et al. (2010) and references therein.

364

365 5. Results

366 5.1. Ballachulish Slate Formation samples

367 The Ballachulish Slate samples have Re (0.3 – 1.9 ppb) and Os (25.5 – 52.2 ppt)
368 abundances that are close to or less than that of average continental crustal values of ~1
369 ppb and 50 ppt, respectively (Table 1; Esser and Turekian, 1993; Peucker-Ehrenbrink and
370 Jahn, 2001; Hattori et al., 2003; Sun et al., 2003). The $^{187}\text{Re}/^{188}\text{Os}$ ratios range from 56.5
371 to 311.7 and the $^{187}\text{Os}/^{188}\text{Os}$ ratios range from 1.660 – 4.478 (Table 1). Regression of the
372 Re-Os isotope data yields a Re-Os age of 659.6 ± 9.6 Ma (2σ , $n = 5$, Model 1, Mean
373 Square of Weighted Deviates [MSWD] = 0.01, initial $^{187}\text{Os}/^{188}\text{Os} = 1.04 \pm 0.03$; Fig. 3a).

374 Digestion of the Ballachulish samples using inverse *aqua-regia* yields elemental
375 abundances of 0.3 – 1.8 ppb and 30.6 – 53.5 ppt for Re and Os, respectively, which are
376 identical within uncertainty to the values from the samples digested using $\text{CrO}_3\text{-H}_2\text{SO}_4$
377 (Table 1). The $^{187}\text{Re}/^{188}\text{Os}$ ratios range from 41.4 to 308.2 and the $^{187}\text{Os}/^{188}\text{Os}$ ratios range
378 from 1.472 to 4.364 (Table 1). Regression of the *aqua-regia* derived Re-Os isotope data
379 yields a Model 3 age of 655 ± 49 Ma (2σ , $n = 5$, MSWD = 16) with an initial Os isotope
380 composition of 1.03 ± 0.16 (Fig. 3b).

381

382 5.2. Leny Limestone slate samples

383 The Leny Limestone slates are enriched in Re (46.2 – 66.1 ppb) and Os (419 – 633
384 ppt) in comparison to average continental crustal values of ~1 ppb and 50 ppt,

385 respectively (Table 1). The $^{187}\text{Re}/^{188}\text{Os}$ ratios range from 898.4 to 1228.0 and the
386 $^{187}\text{Os}/^{188}\text{Os}$ ratios range from 6.162 – 8.075 (Table 1). Regression of the Re-Os isotope
387 data yields a Re-Os age of 310 ± 110 Ma (2σ , $n = 9$, Model 3, MSWD = 388, initial
388 $^{187}\text{Os}/^{188}\text{Os} = 1.7 \pm 2.0$; Fig. 4).

389

390 **6. Discussion**

391 *6.1. Effect of non-hydrogenous Re and Os in low abundance samples*

392 The $\text{CrO}_3\text{-H}_2\text{SO}_4$ method has been shown to yield precise and accurate
393 depositional age determinations for both Phanerozoic and Proterozoic sedimentary
394 successions (Kendall et al., 2004; 2006; 2009a, c; Selby and Creaser, 2005; Anbar et al.,
395 2007; Selby, 2007; Yang et al., 2009; Rooney et al., 2010). Data from the Ballachulish
396 samples using the $\text{CrO}_3\text{-H}_2\text{SO}_4$ digestion method yields a Model 1 age with a low
397 uncertainty (1.5 %) and a low degree of scatter about the isochron (MSWD <1).
398 However, as these samples have Re and Os abundances comparable to that of average
399 continental crust it is important to assess the effects of a detrital Re and Os component on
400 the geochronology data. It has been shown that the incorporation of a detrital Os
401 component could lead to a younger or older age depending on the isotopic composition of
402 the detrital Os (Ravizza et al., 1991). The effects of a detrital Os component on Re-Os
403 depositional ages have been assessed previously during the development of the $\text{CrO}_3\text{-}$
404 H_2SO_4 method (Selby and Creaser, 2003; Kendall et al., 2004).

405 The results from the inverse *aqua-regia* digestion show Re and Os abundances
406 that are comparable with the samples digested using $\text{CrO}_3\text{-H}_2\text{SO}_4$ (Table 1). The isotopic
407 composition data highlights the impact of detrital Re and Os on the determination of
408 depositional ages. All of the $^{187}\text{Re}/^{188}\text{Os}$ and $^{187}\text{Os}/^{188}\text{Os}$ values for the *aqua-regia*
409 samples are lower than those of the samples digested using $\text{CrO}_3\text{-H}_2\text{SO}_4$ (15% and 9%
410 lower, respectively; Table 1). This suggests that the *aqua-regia* digestion has liberated an
411 unradiogenic detrital Os component. Both ages for the Ballachulish Slate Formation are
412 very similar however, however the *aqua-regia* Re-Os data set have a much larger degree
413 of scatter (MSWD = 16) and yield a less precise age (9% uncertainty; Fig 3b, c). The
414 samples digested using the $\text{CrO}_3\text{-H}_2\text{SO}_4$ method yield a much more precise age with a
415 lower degree of scatter (MSWD = 0.01; Fig. 3a). These variations in precision and
416 geological scatter are very similar to those identified by previous studies which undertook

417 digestion of samples in *aqua-regia* (Selby and Creaser, 2003; Kendall et al., 2004).
418 Additionally, digesting samples in the $\text{CrO}_3\text{-H}_2\text{SO}_4$ solution at 80 °C instead of 220 °C
419 has been shown to yield identical data supporting the notion that this method does not
420 liberate non-hydrogenous Re and Os even at high temperatures (Kendall et al., 2009a).

421 The $^{187}\text{Os}/^{188}\text{Os}$ initial ratio (Os_i) data from the samples digested using the $\text{CrO}_3\text{-}$
422 H_2SO_4 method are all very similar with a coefficient of variation of 0.3% in contrast to
423 the Os_i data from the samples digested in *aqua-regia* which have a coefficient of
424 variation of 5% (coefficient of variation = $(\text{SD}/\text{mean}) \times 100$; Table 1). This suggests that
425 there were variations in Os isotope composition and / or magnitude of the detrital Os flux
426 into the Ballachulish Slate during deposition. Again, this is identical to the findings of
427 Kendall et al. (2004) on the Old Fort Point Formation of Canada.

428 The low degree of scatter coupled with the precise age of 659.6 ± 9.6 Ma
429 represents a depositional age for the Ballachulish Slate Formation and the initial
430 $^{187}\text{Os}/^{188}\text{Os}$ isotope composition of 1.04 represents that of seawater at the time of
431 deposition.

432

433 *6.2. Implications for low Re and Os abundance geochronology*

434 The Re-Os age for the Ballachulish Slate Formation indicate that samples with low
435 Re and Os abundances (<1 ppb Re and <50 ppt Os) can be used to provide precise
436 geochronological data (Fig. 3a; Table 1). These values are similar to abundances in
437 average continental crust which range from 0.2 – 2 ppb and 30 – 50 ppt, respectively
438 (Esser and Turekian, 1993; Peucker-Ehrenbrink and Jahn, 2001; Hattori et al., 2003; Sun
439 et al., 2003).

440 Previous work on Re-Os geochronology has focused on sedimentary units greatly
441 enriched in Re and Os with abundances >20 ppb and 500 ppt, respectively (Ravizza et al.,
442 1989; Cohen et al., 1999, Creaser et al., 2002; Selby and Creaser, 2005; Selby, 2007;
443 Rooney et al., 2010). However, some recent studies have successfully applied the Re-Os
444 geochronometer to sedimentary rocks with low to moderate enrichments of Re and Os
445 (1.7 – 50 ppb and 82 – 250 ppt, respectively; Kendall et al., 2004; 2006; 2009a, b; Yang
446 et al., 2009). The Re-Os geochronology data for the Ballachulish Slate Formation
447 represent successful application of the system to samples with very low Re and Os
448 abundances provided that the system has not been disturbed as discussed below.

449 The low Re and Os abundances do not appear to impair the robustness of the system
450 as the Ballachulish samples all have similar $^{187}\text{Os}/^{188}\text{Os}$ (Os_i) values, yield a large spread
451 in present-day $^{187}\text{Re}/^{188}\text{Os}$ values (~ 260 units) and display positively correlated,
452 radiogenic $^{187}\text{Os}/^{188}\text{Os}$ values indicative of a closed system (Table 1). This positive
453 correlation indicates that the 659.6 ± 9.6 Ma age for the Ballachulish Slate Formation
454 does not represent a mixing line. Additionally, if the systematics had been disturbed, any
455 detrital Os component in these samples would represent a significant cause of geological
456 uncertainty, resulting in an imprecise and geologically meaningless age. The highly
457 precise age coupled with the low degree of scatter in the data, (659.6 ± 9.6 and $\text{MSWD} =$
458 0.01), suggests that this is a depositional age and the Os_i value of 1.04 represents the Os
459 isotope composition of local seawater at the time of deposition. The results from the
460 Ballachulish Slate Formation strongly suggest that the system can be applied to
461 sedimentary units that have low Re and Os abundances. From this we can also propose
462 that the system is robust enough to provide depositional ages for strata that have
463 experienced complex and polyphase metamorphic histories.

464

465 6.3. Age of the Ballachulish Slate Formation

466 The Re-Os isotope data from the Ballachulish slates yield an age of 659.6 ± 9.6 Ma
467 which represents the depositional age of the Ballachulish Slate Formation (Fig. 3a).
468 Accordingly, this Re-Os age defines a maximum age constraint for the glaciogenic Port
469 Askaig Formation (Fig. 2). Taken in the context of the previous geochronological
470 constraints for the Dalradian, the Re-Os age for the Ballachulish Slate Formation strongly
471 suggests that the Argyll Group was deposited within ~ 60 Ma, prior to the eruption of the
472 Tayvallich volcanics at ca. 600 Ma. From these two geochronological constraints,
473 combined with the possibility that correlatives of the ca. 635 Ma Marinoan cap carbonate
474 sequence are found within units of the Easdale Subgroup (McCay et al., 2006) we suggest
475 that the Port Askaig Formation records a low latitude glacial event that occurred at ca.
476 650 Ma.

477 Much of the recent work relating to the Dalradian Supergroup has focused on $\delta^{13}\text{C}$
478 carbonate and $^{87}\text{Sr}/^{86}\text{Sr}$ chemostratigraphy of the various carbonate units (Prave et al.,
479 2009a and references therein; Sawaki et al., 2010). This focus on chemostratigraphy
480 coupled with the lack of reliable geochronology data has resulted in several attempts at

481 correlation of the Dalradian Supergroup with better constrained Neoproterozoic
482 sequences (McCay et al., 2006; Prave et al., 2009a; Sawaki et al., 2010). The Ballachulish
483 Limestone is ca. 200 m in thickness and passes upwards into the Ballachulish Slate
484 (Anderton, 1982; Prave et al., 2009a). Work by Prave et al. (2009a) suggested that the
485 Ballachulish Limestone possess $\delta^{13}\text{C}_{\text{carbonate}}$ values as low as -7‰ and was tentatively
486 correlated with the ca. 800 Ma Bitter Springs anomaly of central Australia (Hill and
487 Walter, 2000; Halverson et al., 2007b). However, the Re-Os data of 659.6 ± 9.6 Ma for
488 the Ballachulish Slate Formation negates the possibility of this correlation (Fig. 2).

489 A 60 Ma duration for Argyll Group deposition suggested by the Re-Os data presented
490 here contrasts with a duration of ca. 120 Ma required by chemostratigraphic and
491 lithostratigraphic correlations of the Port Askaig Formation with a ca. 715 Ma “Sturtian”
492 glacial (Prave, 1999; Brasier and Shields, 2000; Prave et al., 2009a;). A short duration for
493 Argyll Group deposition is geologically more probable given that the Argyll Group
494 represents a time of increased tectonic activity and syn-depositional faulting with rapid
495 deposition taking place in subsiding fault-bounded sub-basins (Anderton, 1982; 1985). A
496 short duration for Argyll Group deposition also negates the need for any putative
497 regional-scale unconformity within the Argyll Group, which remains contentious (see
498 Hutton and Alsop, 2004 and Tanner et al., 2005 for a review).

499 The new Re-Os geochronology data provide a more precise chronostratigraphic
500 framework for understanding the tectonic evolution of the Dalradian basin and the onset
501 of sedimentation within the basin. Furthermore, the Re-Os geochronology helps refine
502 Neoproterozoic palaeogeographies related to the formation and breakup of the Rodinia
503 supercontinent (e.g., Li et al., 2008; Li and Evans, 2010). Deposition of the Dalradian
504 Supergroup occurred along the eastern margin of Laurentia, close to the triple junction of
505 Baltica, Laurentia and Amazonia (Soper, 1994; Dalziel, 1994).

506

507 *6.4. Implications for global correlations involving the glacial Port Askaig Formation*

508 At present, global correlation schemes for Neoproterozoic glaciogenic deposits are
509 dependent on correlation of two distinctive types of diamictite cap-carbonate pairs. These
510 have been designated as “Sturtian” and “Marinoan” events after the type localities in
511 southern Australia (Kennedy et al., 1998; Hoffman and Schrag, 2002; Halverson et al.,
512 2005; Corsetti and Lorentz, 2006). The Sturtian glaciation however, is also used to define

513 much older glacial events than the Sturtian *sensu stricto* of the Adelaide Rift Complex
514 which has geochronological constraints of ca. 640 – 660 Ma (Preiss, 2000; Kendall et al.,
515 2009a and references therein). These earlier glacial events assigned to the “Sturtian” have
516 geochronological constraints which indicate low-latitude global glaciation at ca. 715 Ma
517 based on U-Pb zircon ages (Bowring et al., 2007; Macdonald et al., 2010a). In this
518 summary, they are referred to as middle Cryogenian (ca. 715 Ma) deposits to distinguish
519 them from younger Sturtian (*sensu stricto*) glacial deposits on the Australian craton at ca.
520 640 – 660 Ma.

521 Early work on correlation of the Port Askaig Formation (Fig. 2) suggested a possible
522 correlation with North Atlantic Varangerian tillite sequences which were originally
523 constrained by a Rb-Sr diagenetic illite age of ca. 630 Ma (Hambrey, 1983; Fairchild and
524 Hambrey, 1995; Gorokhov et al., 2001). Correlation of the Port Askaig Formation with
525 the Varangerian tillite was also suggested by $^{87}\text{Sr}/^{86}\text{Sr}$ chemostratigraphy of Dalradian
526 limestones that indicate that the base of the Dalradian Supergroup is younger than ca. 800
527 Ma and may be as young as ca. 700 Ma (Thomas et al., 2004). This correlation is difficult
528 to support as the geochronological constraints for the Varangerian glaciation are based
529 upon Rb-Sr illite geochronology, which is unlikely to represent a depositional age
530 (Morton and Long, 1982; Ohr et al., 1991; Awwiller, 1994; Evans, 1996; Gorokhov et al.,
531 2001; Selby, 2009).

532 Recent work has rejected the correlation of the Port Askaig Formation and the
533 Varangerian glaciation. Instead, $\delta^{13}\text{C}$ and $^{87}\text{Sr}/^{86}\text{Sr}$ profiles from the underlying Islay
534 Limestone and overlying Bonahaven Formation have been used to suggest a middle
535 Cryogenian (ca. 715 Ma) age for the Port Askaig Formation (Brasier and Shields, 2000;
536 Prave et al., 2009a). Further ‘evidence’ for a 715 Ma middle Cryogenian age for the Port
537 Askaig Formation is the presence of younger glaciogenic units in the Dalradian, namely
538 the Stralinchy-Reelan (a possible Marinoan correlative) and the Inishowen-Loch na Cille
539 Formations (a possible Gaskiers correlative; Condon and Prave, 2000; McCay et al.,
540 2006). However, the Re-Os age of 659.6 ± 9.6 Ma for the Ballachulish Slate Formation
541 refutes the notion that the Port Askaig Formation is a component of a middle Cryogenian
542 (ca. 715 Ma) glaciation. As reported above, the Re-Os age, coupled with existing
543 geochronology constraints on the Tayvallich volcanics strongly suggest that the Port
544 Askaig Formation records a glacial event on the eastern margin of Laurentia at ~650 Ma.

545 Palaeomagnetic constraints from Laurentia during the Neoproterozoic indicate that
546 Laurentia (and hence the Port Askaig Formation) was at low latitudes from 723 – 614 Ma
547 (see Trinidade and Macouin, 2007 and references therein). Similarly, the Sturtian (*sensu*
548 *stricto*) glaciations on the Australian craton were also at low latitude and Re-Os
549 geochronology of post-glacial rocks indicates an age of ~650 Ma for these glacial
550 deposits. The Ballachulish Slate Formation Re-Os geochronology implies that the Port
551 Askaig Formation could be correlated with the ~650 Ma Sturtian (*sensu stricto*) deposits
552 of the Adelaide Rift Complex (Preiss, 2000; Kendall et al., 2006; 2009a). This suggestion
553 is also supported by the Os_i data for the Ballachulish Slate, Upper Black River Dolomite
554 and Tapley Hill formations as discussed below (Fig. 5; Kendall et al., 2006; 2009a; This
555 study).

556

557 6.5. *Os isotopic composition of seawater at 660 Ma*

558 The initial Os_i values determined from the regression of the Re-Os isotope data
559 (Table 1; Figs. 3 and 4) are interpreted to reflect the Os isotope composition of seawater
560 at the time of deposition (Ravizza and Turekian, 1989; Cohen et al., 1999; Selby and
561 Creaser, 2003). The Os isotope composition for seawater at the time of deposition of the
562 Ballachulish Slate (1.04 ± 0.03) is identical, within uncertainty, to that of the present day
563 Os isotopic composition of seawater (~1.06; [Peucker-Ehrenbrink and Ravizza, 2000](#) and
564 references therein; Rooney et al., unpublished data). The radiogenic Os_i value from the
565 Ballachulish Slate Formation suggests that the contribution of radiogenic Os from
566 riverine inputs and weathering of upper continental crustal material (present-day riverine
567 inputs of $^{187}Os/^{188}Os \sim 1.5$; [Levasseur et al., 1999](#)) dominated over the influx of
568 unradiogenic Os from cosmic dust and hydrothermal alteration of oceanic crust and
569 peridotites (present-day $^{187}Os/^{188}Os \sim 0.13$; [Walker et al., 2002a, b](#)).

570 The radiogenic values for the Os_i of the Ballachulish Slate Formation closely
571 match values for the post-glacial Upper Black River Dolomite, Aralka and Tapley Hill
572 Formations of southern Australia (1.04; 1.00; 0.82; 0.95, respectively; Kendall et al.,
573 2006; 2009a). Although there are many contrasting palaeomagnetic reconstructions of the
574 Laurentian and Australian cratons, most models indicate that during the Neoproterozoic
575 these two cratons were both located at low latitudes and were separated by oceanic basins
576 that formed as a result of rifting associated with the breakup of Rodinia (Li et al., 2008

577 and references therein; Li and Evans, 2010). We postulate that the very similar Os_i values
578 reported from the pre-glacial Ballachulish and post-glacial Upper Black River Dolomite,
579 Aralka and Tapley Hill Formations represent a possibly global Os isotope composition
580 for the 660 – 640 Ma time interval (Kendall et al., 2006; 2009a). Additionally, this
581 ‘global’ isotope composition for this interval is significantly more radiogenic than values
582 for Mesoproterozoic seawater Os isotope composition (1.04 compared to 0.33 and 0.29;
583 Rooney et al., 2010 and Kendall et al., 2009c). One possibility is that falling sea levels
584 and the exposure of rifted margins associated with the breakup of Rodinia would expose
585 older, more radiogenic continental crust to weathering. A further explanation for the
586 increase in $^{187}Os/^{188}Os$ isotope composition for the Neoproterozoic is the increased
587 oxygenation of deep waters during the late Neoproterozoic (Canfield and Teske, 1996;
588 Anbar and Knoll, 2002; Canfield et al., 2007; 2008; Scott et al., 2008). This oxygenation
589 of the oceans and atmosphere would result in increased chemical weathering of
590 continental crust which, coupled with the breakup of Rodinia may result in an increase in
591 seawater Os as seen for the Sr isotope composition of Neoproterozoic seawater (Jacobsen
592 and Kaufman, 1999; Halverson et al., 2007a).

593

594 *6.6. Systematics of Re-Os in Leny Limestone Formation*

595 Although the Ballachulish Slate Formation experienced complex and polyphase
596 metamorphism, these samples yield a precise depositional age with a low degree of
597 scatter about the linear regression of the Re-Os data (659.6 ± 9.6 Ma, MSWD = 0.01).
598 The results for the Ballachulish Slate samples imply that anhydrous metamorphism and
599 dehydration reactions do not adversely affect Re-Os systematics. In contrast, the Leny
600 Limestone Formation which has also experienced regional Grampian metamorphic events
601 has been disturbed. We suggest that this Re-Os isotope disturbance is probably related to
602 hydration and fluid-flow events associated with Carboniferous / Permian contact
603 metamorphism as discussed below.

604 The Re-Os isotope data for the Leny Limestone Formation yield a highly imprecise
605 age of 310 ± 110 Ma (MSWD = 338) that is significantly younger than the accepted age
606 of ca. 512 Ma based upon the trilobite fauna found in the Leny Limestone (Fletcher and
607 Rushton, 2007). In addition, the Os_i value of 1.7 ± 2.0 is much more radiogenic than
608 known values for Cambrian seawater (~ 0.8 ; Mao et al., 2002) and all of the Phanerozoic.

609 The Re-Os geochronometer has been shown to be robust following hydrocarbon
610 maturation events, greenschist-facies metamorphism and flash pyrolysis thus suggesting
611 the system is robust even after temperatures as high as 650 °C and pressures as high as 3
612 kbar (Creaser et al., 2002; Kendall et al., 2004; 2006; 2009; Rooney et al., 2010).
613 Disturbance of the Re-Os systematics by chemical weathering has been identified from
614 outcrop studies on the Ohio Shale (Jaffe et al., 2002). The Leny Limestone Formation
615 outcrop is not significantly weathered and the samples were taken in such a way as to
616 avoid the effects of recent chemical weathering on the outcrop. The measures undertaken
617 to ensure that fresh samples were used for Re-Os geochronology include; removal of
618 surficial weathering prior to sampling of large (~200 g) samples extracted from the
619 outcrop prior to cutting which meant that any evidence of weathering e.g., iron-staining
620 or leaching and features such as quartz veins could be scrupulously avoided. Thus we do
621 not consider these factors to have played a role in the Re-Os analysis of the Leny
622 Limestone Formation.

623 Recent work has shown that the Re-Os geochronometer is susceptible to disturbance
624 caused by hydrothermal fluid interaction with sedimentary units associated with the
625 formation of a SEDEX deposit (Kendall et al., 2009c). The proximity of the Leny
626 Limestone exposures to the Devonian and Permo-Carboniferous intrusions and associated
627 interactions with hydrothermal fluids are likely causes of disturbance of the Re-Os
628 systematics. In agreement with work by Kendall et al. (2009c) we suggest that the Re-Os
629 age for the Leny Limestone represents a disturbed dataset. The negative Os_i values
630 calculated at 512 Ma and the anomalously young age can be best explained by post-
631 depositional mobilization of Re and Os resulting from hydrothermal fluid flow driven by
632 the igneous intrusions found within the Leny Quarry. Possibly oxidising fluids generated
633 by the intrusions may have leached Re and/or Os from the Leny Slate samples. The Leny
634 Limestone slate samples all have $^{187}Re/^{188}Os$ values that plot to the right of the 512 Ma
635 reference line suggestive of either Re gain or Os loss (Fig. 5). The occurrence of
636 kaolinite, muscovite and berthierine from XRD analysis of the Leny Limestone
637 Formation slates suggests that these minerals are the products of retrograde reactions
638 involving chlorite, muscovite and an Fe-rich phase such as cordierite that was driven by
639 reactions with hydrothermal fluids (Slack et al., 1992; Abad et al., 2010).

640 The lack of documented mineralisation (small [<1 cm thick] dolomite veins in the
641 limestones notwithstanding) and identifiable accessory or index minerals renders it
642 extremely challenging to gain a full understanding of the P-T conditions of contact
643 metamorphism in the Leny Limestone Formation. However, given that the Grampian
644 Orogeny would have generated local greenschist-facies conditions it is likely that
645 hydrothermal fluid flow driven by the Palaeozoic igneous intrusions hydrated the Leny
646 Limestone slates resulting in retrograde reactions and the disturbance of the Re-Os
647 geochronometer.

648

649 **7. Conclusions**

650 New Re-Os geochronology for the Ballachulish Slate Formation yields a depositional
651 age of 659.6 ± 9.6 Ma providing a maximum age constraint for the overlying glaciogenic
652 Port Askaig Formation. The precise age coupled with the excellent linear fit of the Re-Os
653 isotope data for the Ballachulish Slate Formation represents the first successful
654 application of the Re-Os system in samples with Re and Os abundances comparable with,
655 or lower than, average continental crustal values. Additionally, these results strongly
656 suggest that meaningful Re-Os geochronology data can be obtained from sedimentary
657 successions that have experienced polyphase contact and regional metamorphism
658 provided that thermal alteration was anhydrous.

659 The Re-Os geochronology presented here indicates that the Port Askaig Formation is
660 much younger than the middle Cryogenian glacial horizons bracketed at ca. 750 – 690
661 Ma, with which it was previously correlated. The new geochronology data for the
662 Ballachulish Slate Formation also refutes a correlation of the underlying Ballachulish
663 Limestone Formation with the ca. 800 Ma Bitter Springs anomaly of Australia (Hill and
664 Walter, 2000; Halverson et al., 2007b; Prave et al., 2009a). The Re-Os geochronology
665 provides a chronostratigraphic framework that indicates deposition of the Argyll Group
666 occurred within a ~ 60 Ma interval prior to eruption of the Tayvallich Volcanics. The Re-
667 Os data provide further support for the argument that Re-Os and U-Pb zircon
668 geochronology are fundamental if we are to use chemostratigraphy to evaluate
669 Neoproterozoic environments.

670 The Os_i value for seawater at the time of deposition of the Ballachulish Slate
671 Formation is similar to that of the present-day value indicating that the dominant input of

672 Os to seawater was radiogenic input from the weathering of the continental crust.
673 Additionally, the close similarity of Os_i values from the Ballachulish Slate Formation
674 with Sturtian (*sensu stricto*) deposits from the Australian craton indicates that the
675 dominant source of Os to the oceans was from weathering of an evolved upper
676 continental crust.

677 Disturbance of Re-Os systematics in the Leny Limestone Formation is evident by a
678 very imprecise and inaccurate age along with a negative value for the Os_i value
679 (calculated at 512 Ma) for seawater in this biostratigraphically constrained Cambrian
680 unit. These factors strongly suggest that the Re-Os system was disturbed in response to
681 hydrothermal fluid flow associated with the intrusion of a number of igneous bodies
682 during the Palaeozoic. The circulation of fluids through the Leny Limestone Formation is
683 suggested to be the cause for the gain of Re and / or the loss of Os thus generating an
684 imprecise age younger than the known depositional age.

685

686 **Acknowledgements**

687 This research was funded by a TOTAL CeREES PhD scholarship awarded to
688 ADR. Maggie White is thanked for her assistance with the XRD work. We would like to
689 thank Rob Strachan, Tony Prave, and Alex Finlay for discussions on Dalradian geology
690 and Re-Os systematics. Constructive criticism from Graham Shields and an anonymous
691 reviewer also further improved this manuscript. The TOTAL laboratory for source rock
692 geochronology and geochemistry at NCIET is partly funded by TOTAL.

693 **References:**

- 694 Abad, I., Murphy, B., Nieto, F., Guiterrez-Alonso, G., 2010. Diagenesis to
695 metamorphism transition in an episutural basin: the late Paleozoic St. Mary's
696 Basin, Nova Scotia, Canada. *Canadian Journal of Earth Sciences*, **47**, 121-135.
- 697 Anbar, A. D., Knoll, A. H., 2002. Proterozoic ocean chemistry and evolution: A
698 bioinorganic bridge? *Science* **297**, 1137-1142.
- 699 Anbar, A.D., Duan, Y., Lyons, T.W., Arnold, G.L., Kendall, B., Creaser, R.A., Kaufman,
700 A.J., Gordon, G.W., Scott, C., Garvin, J., Buick, R. 2007. A whiff of oxygen
701 before the Great Oxidation Event? *Science*, **317**, 1903 - 1906.
- 702 Anderton, R., 1982. Dalradian deposition and the late Precambrian-Cambrian history of
703 the N Atlantic region: a review of the early evolution of the Iapetus Ocean.
704 *Journal of the Geological Society* **139**, 421-431.
- 705 Anderton, R., 1985. Sedimentation and tectonics in the Scottish Dalradian. *Scot J Geol*
706 **21**, 407-436.
- 707 Arnaud, E., Eyles, C. H., 2002. Catastrophic mass failure of a Neoproterozoic glacially
708 influenced continental margin, the Great Breccia, Port Askaig Formation,
709 Scotland. *Sedimentary Geology* **151**, 313-333.
- 710 Arnaud, E., 2004. Giant cross-beds in the Neoproterozoic Port Askaig Formation,
711 Scotland: implications for snowball Earth. *Sedimentary Geology* **165**, 155-174.
- 712 Awwiller, D.N., 1994 Geochronology and Mass-Transfer in Gulf-Coast Mudrocks
713 (South-Central Texas, USA) - Rb-Sr, Sm-Nd and Ree Systematics. *Chemical*
714 *Geology*, **116**, 61-84.
- 715 Baker, A. J., 1985. Pressures and temperatures of metamorphism in the eastern Dalradian.
716 *Journal of the Geological Society* **142**, 137-148.
- 717 Banks, C.J., Smith, M., Winchester, J.A., Horstwood, M.S.A., Noble, S.R., Ottley, C.J.,
718 2007. Provenance of intra-Rodinian basin-fills: The Lower Dalradian Supergroup,
719 Scotland. *Precambrian Research* **153**, 46-64.
- 720 Barrow, G., 1893. On an intrusion of muscovite-biotite gneiss in the southeast Highlands
721 of Scotland and its accompanying metamorphism. *Quarterly Journal of the*
722 *Geological Society of London* **19**, 330-358.
- 723 Baxter, E. F., Ague, J. J., Depaolo, D. J., 2002. Prograde temperature-time evolution in
724 the Barrovian type-locality constrained by Sm/Nd garnet ages from Glen Clova,
725 Scotland. *Journal of the Geological Society* **159**, 71-82.
- 726 Bowring, S., Myrow, P., Landing, E., Ramezani, J., Grotzinger, J., 2003.
727 Geochronological constraints on terminal Neoproterozoic events and the rise of
728 metazoans: Geophysical Research Abstracts. **5**, p.13219.
- 729 Bowring, S. A., Grotzinger, J. P., Condon, D. J., Ramezani, J., Newall, M. J., Allen, P.
730 A., 2007. Geochronologic constraints on the chronostratigraphic framework of the
731 Neoproterozoic Huqf Supergroup, Sultanate of Oman. *Am J Sci* **307**, 1097-1145.
- 732 Brasier, M. D., Shields, G., 2000. Neoproterozoic chemostratigraphy and correlation of
733 the Port Askaig glaciation, Dalradian Supergroup of Scotland. *Journal of the*
734 *Geological Society* **157**, 909-914.
- 735 British Geological Survey, 2005. Aberfoyle. Scotland Sheet 38E. Bedrock and
736 Superficial geology. 1:50 000. Geology Series. British Geological Survey,
737 Keyworth, Nottingham
- 738 Brindley, G.W., 1982. Chemical compositions of berthierines, a review. *Clays and Clay*
739 *Minerals*, **30**, 153-155.

- 740 Canfield, D.E., Teske, A., 1996. Late Proterozoic rise in atmospheric oxygen
741 concentration inferred from phylogenetic and sulphur-isotope studies. *Nature* **382**,
742 127-132.
- 743 Canfield, D.E., Poulton, S.W., Narbonne, G.M., 2007. Late-Neoproterozoic Deep-Ocean
744 Oxygenation and the Rise of Animal Life. *Science* **315**, 92-95.
- 745 Canfield, D. E., Poulton, S. W., Knoll, A. H., Narbonne, G. M., Ross, G., Goldberg, T.,
746 Strauss, H., 2008. Ferruginous Conditions Dominated Later Neoproterozoic
747 Deep-Water Chemistry. *Science* **321**, 949-952.
- 748 Cawood, P. A., Nemchin, A. A., Smith, M., Loewy, S., 2003. Source of the Dalradian
749 Supergroup constrained by U-Pb dating of detrital zircon and implications for the
750 East Laurentian margin. *Journal of the Geological Society* **160**, 231-246.
- 751 Cawood, P. A., Nemchin, A. A., Strachan, R., Prave, T., Krabbendam, M., 2007.
752 Sedimentary basin and detrital zircon record along East Laurentia and Baltica
753 during assembly and breakup of Rodinia. *Journal of the Geological Society* **164**,
754 257-275.
- 755 Cawood, P. A., Nemchin, A. A., Strachan, R. A., Kinny, P. D., Loewy, S., 2004.
756 Laurentian provenance and an intracratonic tectonic setting for the Moine
757 Supergroup, Scotland, constrained by detrital zircons from the Loch Eil and Glen
758 Urquhart successions. *Journal of the Geological Society* **161**, 861-874.
- 759 Chew, D. M., Fallon, N., Kennelly, C., Crowley, Q., Pointon, M., 2010. Basic volcanism
760 contemporaneous with the Sturtian glacial episode in NE Scotland. *T Roy Soc*
761 *Edin-Earth*.
- 762 Cohen, A. S., Coe, A. L., Bartlett, J. M., Hawkesworth, C. J., 1999. Precise Re-Os ages of
763 organic-rich mudrocks and the Os isotope composition of Jurassic seawater. *Earth*
764 *and Planetary Science Letters* **167**, 159-173.
- 765 Condon, D. J., Prave, A. R., 2000. Two from Donegal: Neoproterozoic glacial episodes
766 on the northeast margin of Laurentia. *Geology* **28**, 951-954.
- 767 Condon, D., Zhu, M., Bowring, S., Wang, W., Yang, A., Jin, Y., 2005. U-Pb Ages from
768 the Neoproterozoic Doushantuo Formation, China. *Science*, **308**, 95-98.
- 769 Conliffe, J., Selby, D., Porter, S. J., Feely, M., 2010. Re-Os molybdenite dates from the
770 Ballachulish and Kilmelford Igneous Complexes (Scottish Highlands): age
771 constraints for late Caledonian magmatism. *Journal of the Geological Society*
772 **167**, 297-302.
- 773 Corsetti, F. A., Lorentz, N. J., 2006. On Neoproterozoic Cap Carbonates as
774 Chronostratigraphic Markers. In: Xiao, S., Kaufman, A. J., (Eds.), Neoproterozoic
775 Geobiology and Paleobiology. Springer, New York, pp. 273-294.
- 776 Creaser, R. A., Sannigrahi, P., Chacko, T., Selby, D., 2002. Further evaluation of the Re-
777 Os geochronometer in organic-rich sedimentary rocks: A test of hydrocarbon
778 maturation effects in the Exshaw Formation, Western Canada Sedimentary Basin.
779 *Geochimica et Cosmochimica Acta* **66**, 3441-3452.
- 780 Dalziel, I. W. D., 1994. Precambrian Scotland as a Laurentia-Gondwana Link - Origin
781 and Significance of Cratonic Promontories. *Geology* **22**, 589-592.
- 782 Dalziel, I. W. D., Soper, N. J., 2001. Neoproterozoic Extension on the Scottish
783 Promontory of Laurentia: Paleogeographic and Tectonic Implications. *The*
784 *Journal of Geology* **109**, 299-317.
- 785 Dempster, T. J., 1992. Zoning and recrystallization of phengitic micas: implications for
786 metamorphic equilibration. *Contrib. Mineral Petr.* **109**, 526-537.

- 787 Dempster, T.J., Rogers, G., Tanner, P.W.G., Bluck, B.J., Muir, R.J., Redwood, S.D.,
788 Ireland, T. R., Paterson, B. A., 2002. Timing of deposition, orogenesis and
789 glaciation within the Dalradian rocks of Scotland: constraints from U-Pb zircon
790 ages. *Journal of the Geological Society* **159**, 83-94.
- 791 Dewey, J., Mange, M., 1999. Petrography of Ordovician and Silurian sediments in the
792 western Irish Caledonides: tracers of a short-lived Ordovician continent-arc
793 collision orogeny and the evolution of the Laurentian Appalachian-Caledonian
794 margin. *Geological Society, London, Special Publications* **164**, 55-107.
- 795 Esser, B. K., Turekian, K. K., 1993. The osmium isotopic composition of the continental
796 crust. *Geochimica Cosmochimica Acta* **57**, 3093-3104.
- 797 Evans, J.A., 1996. Dating the transition of smectite to illite in Palaeozoic mudrocks using
798 the Rb-Sr whole-rock technique. *Journal of the Geological Society*, **153**, 101-108.
- 799 Evans, D. A. D., 2000. Stratigraphic, geochronological, and paleomagnetic constraints
800 upon the Neoproterozoic climatic paradox. *Am J Sci* **300**, 347-433.
- 801 Eyles, C. H., 1988. Glacially-Influenced and Tidally-Influenced Shallow Marine
802 Sedimentation of the Late Precambrian Port Askaig Formation, Scotland.
803 *Palaeogeography Palaeoclimatology Palaeoecology* **68**, 1-25.
- 804 Fairchild, I. J. Hambrey, M. J., 1995. Vendian basin evolution in East Greenland and NE
805 Svalbard. *Precambrian Research* **73**, 217-233.
- 806 Fairchild, I. J., Kennedy, M. J., 2007. Neoproterozoic glaciation in the Earth System.
807 *Journal of the Geological Society* **164**, 895-921.
- 808 Fanning, C.M., Link, P.K., 2004. U-Pb SHRIMP ages of Neoproterozoic (Sturtian)
809 glaciogenic Pocatello Formation, southeastern Idaho. *Geology*, **32**, 881-884.
- 810 Fike, D. A., Grotzinger, J. P., Pratt, L. M., Summons, R. E., 2006. Oxidation of the
811 Ediacaran Ocean. *Nature* **444**, 744-747.
- 812 Fletcher, T. P., Rushton, A. W. A., 2007. The Cambrian Fauna of the Leny Limestone,
813 Perthshire, Scotland. *Earth Env. Sci. T. R. So.* **98**, 199-218.
- 814 Friedrich, A. M., Hodges, K. V., Bowring, S. A., Martin, M. W., 1999. Geochronological
815 constraints on the magmatic, metamorphic and thermal evolution of the
816 Connemara Caledonides, western Ireland. *Journal of the Geological Society* **156**,
817 1217-1230.
- 818 Frimmel, H. E., On the reliability of stable carbon isotopes for Neoproterozoic
819 chemostratigraphic correlation. *Precambrian Research* **182** 239-253.
- 820 Giddings, J. A., Wallace, M. W., 2009. Facies-dependent $\delta^{13}\text{C}$ variation from a
821 Cryogenian platform margin, South Australia: Evidence for stratified
822 Neoproterozoic oceans? *Palaeogeography, Palaeoclimatology, Palaeoecology*
823 **271**, 196-214.
- 824 Glover, B. W., Key, R. M., May, F., Clark, G. G., Phillips, E. R., Chacksfield, B. C.,
825 1995. A Neoproterozoic multi-phase rift sequence: the Grampian and Appin
826 groups of the southwestern Monadhliath Mountains of Scotland. *Journal of the*
827 *Geological Society*, **152**, 391-406.
- 828 Glover, B. W., McKie, T., 1996. A sequence stratigraphical approach to the
829 understanding of basin history in orogenic Neoproterozoic successions: an
830 example from the central Highlands of Scotland. *Geological Society, London,*
831 *Special Publications* **103**, 257-269.
- 832 Glover, B. W., Winchester, J. A., 1989. The Grampian Group: a major Late Proterozoic
833 clastic sequence in the Central Highlands of Scotland. *Journal of the Geological*
834 *Society* **146**, 85-96.

- 835 Gorokhov, I. M., Semikhatov, M. A., Mel'nikov, N. N., Turchenko, T. L., Konstantinova,
836 G. V., Kut'yavin, E. P., 2001. Rb-Sr geochronology of middle Riphean shales, the
837 Yusmastakh Formation of the Anabar Massif, northern Siberia. *Stratigr Geo*
838 *Correl+* **9**, 213-231.
- 839 Halliday, A. N., Graham, C. M., Aftalion, M., Dymoke, P., 1989. The Depositional Age
840 of the Dalradian Supergroup - U-Pb and Sm-Nd Isotopic Studies of the Tayvallich
841 Volcanics, Scotland. *Journal of the Geological Society* **146**, 3-6.
- 842 Halverson, G. P., Hoffman, P. F., Schrag, D. P., Maloof, A. C., Rice, A. H. N., 2005.
843 Toward a Neoproterozoic composite carbon-isotope record. *Geological Society of*
844 *America Bulletin* **117**, 1181-1207.
- 845 Halverson, G. P., Hurtgen, M. T., 2007. Ediacaran growth of the marine sulfate reservoir.
846 *Earth and Planetary Science Letters* **263**, 32-44.
- 847 Halverson, G.P., Dudás, F.Ö., Maloof, A.C., Bowring, S.A., 2007a. Evolution of the
848 $^{87}\text{Sr}/^{86}\text{Sr}$ composition of Neoproterozoic seawater. *Palaeogeography,*
849 *Palaeoclimatology, Palaeoecology* **256**, 103-129.
- 850 Halverson, G. P., Maloof, A. C., Schrag, D. P., Dudás, F. Ö., Hurtgen, M., 2007b.
851 Stratigraphy and geochemistry of a ca 800 Ma negative carbon isotope interval in
852 northeastern Svalbard. *Chemical Geology* **237**, 5-27.
- 853 Hambrey, M. J., 1983. Correlation of Late Proterozoic tillites in the North Atlantic region
854 and Europe. *Geological Magazine* **120**, 209-232.
- 855 Harris, A. L., Haselock, P.J., Kennedy, M.J., Mendum, J.R., Long, C.B., Winchester, J.A.
856 Tanner, P.W.G., 1994. The Dalradian Supergroup in Scotland and Ireland. In:
857 Gibbons, W., Harris, A.L. (Ed.), *A Revised correlation of Precambrian rocks in*
858 *the British Isles*. Geological Society, London.
- 859 Harte, B., Pattison, D.R.M., Heuss-Assbichler, S., Hoernes, S., Masch, L., Strong, D.F.,
860 1991. Evidence of fluid phase behaviour and controls in the intrusive complex and
861 its aureole. In: Voll, G., Topel, J., Pattison, D.R.M., Seifert, F. (Ed.), *Equilibrium*
862 *and Kinetics in Contact Metamorphism: the Ballachulish Igneous Complex and*
863 *its Thermal Aureole*. Springer Verlag, Heidelberg.
- 864 Hattori, Y., Suzuki, K., Honda, M., Shimizu, H., 2003. Re-Os isotope systematics of the
865 Taklimakan Desert sands, moraines and river sediments around the taklimakan
866 desert, and of Tibetan soils. *Geochimica Et Cosmochimica Acta* **67**, 1203-1213.
- 867 Highton, A.J., Hyslop, E.K., Noble, S.R., 1999. U-Pb zircon geochronology of
868 migmatization in the northern Central Highlands: evidence for pre-Caledonian
869 (Neoproterozoic) tectonometamorphism in the Grampian block, Scotland. *Journal*
870 *of the Geological Society* **156**, 1195-1204.
- 871 Hill, A. C., Walter, M. R., 2000. Mid-Neoproterozoic (~830-750 Ma) isotope stratigraphy
872 of Australia and global correlation. *Precambrian Research* **100**, 181-211.
- 873 Hoffman, P. F., 1991. Did the Breakout of Laurentia Turn Gondwanaland Inside-Out?
874 *Science* **252**, 1409-1412.
- 875 Hoffman, P. F., Kaufman, A. J., Halverson, G. P., Schrag, D. P., 1998. A Neoproterozoic
876 snowball earth. *Science* **281**, 1342-1346.
- 877 Hoffman, P. F., Schrag, D. P., 2002. The snowball Earth hypothesis: testing the limits of
878 global change. *Terra Nova* **14**, 129-155.
- 879 Hoffmann, K. H., Condon, D. J., Bowring, S. A., Crowley, J. L., 2004. U-Pb zircon date
880 from the Neoproterozoic Ghaub Formation, Namibia: Constraints on Marinoan
881 glaciation. *Geology* **32**, 817-820.

- 882 Hutton, D. H. W., Alsop, G. I., 2004. Evidence for a major Neoproterozoic orogenic
 883 unconformity within the Dalradian Supergroup of NW Ireland. *Journal of the*
 884 *Geological Society* **161**, 629-640.
- 885 Hyde, W. T., Crowley, T. J., Baum, S. K., Peltier, W. R., 2000. Neoproterozoic/snowball
 886 Earth/simulations with a coupled climate/ice-sheet model. *Nature* **405**, 425-429.
- 887 Jacobsen, S.B., Kaufman, A.J., 1999. The Sr, C and O isotopic evolution of
 888 Neoproterozoic seawater. *Chemical Geology* **161**, 37-57.
- 889 Jaffe, L. A., Peucker-Ehrenbrink, B., Petsch, S. T., 2002. Mobility of rhenium, platinum
 890 group elements and organic carbon during black shale weathering. *Earth and*
 891 *Planetary Science Letters* **198**, 339-353.
- 892 Jensen, S., Saylor, B. Z., Gehling, J. G., Germs, G. J. B., 2000. Complex trace fossils
 893 from the terminal Proterozoic of Namibia. *Geology* **28**, 143-146.
- 894 Jiang, G., Kaufman, A. J., Christie-Blick, N., Zhang, S., Wu, H., 2007. Carbon isotope
 895 variability across the Ediacaran Yangtze platform in South China: Implications
 896 for a large surface-to-deep ocean [δ] ^{13}C gradient. *Earth and Planetary*
 897 *Science Letters* **261**, 303-320.
- 898 Kendall, B., Creaser, R. A., Calver, C. R., Raub, T. D., Evans, D. A. D., 2009a.
 899 Correlation of Sturtian diamictite successions in southern Australia and
 900 northwestern Tasmania by Re-Os black shale geochronology and the ambiguity of
 901 "Sturtian"-type diamictite-cap carbonate pairs as chronostratigraphic marker
 902 horizons. *Precambrian Research* **172**, 301-310.
- 903 Kendall, B., Creaser, R. A., Selby, D., 2009b. ^{187}Re - ^{187}Os geochronology of Precambrian
 904 organic-rich sedimentary rocks. *Geological Society, London, Special Publications*
 905 **326**, 85-107.
- 906 Kendall, B., Creaser, R. A., Gordon, G. W., Anbar, A. D., 2009c. Re-Os and Mo isotope
 907 systematics of black shales from the Middle Proterozoic Velkerri and
 908 Wollogorang Formations, McArthur Basin, northern Australia. *Geochimica Et*
 909 *Cosmochimica Acta* **73**, 2534-2558.
- 910 Kendall, B., Creaser, R. A., Selby, D., 2006. Re-Os geochronology of postglacial black
 911 shales in Australia: Constraints on the timing of "Sturtian" glaciation. *Geology* **34**,
 912 729-732.
- 913 Kendall, B. S., Creaser, R. A., Ross, G. M., Selby, D., 2004. Constraints on the timing of
 914 Marinoan 'Snowball Earth' glaciation by ^{187}Re - ^{187}Os dating of a Neoproterozoic
 915 post-glacial black shale in Western Canada. *Earth and Planetary Science Letters*
 916 **222**, 729-740.
- 917 Kennedy, M. J., Runnegar, B., Prave, A. R., Hoffmann, K. H., Arthur, M. A., 1998. Two
 918 or four Neoproterozoic glaciations? *Geology* **26**, 1059-1063.
- 919 Kilburn, C., Shackleton, R. M., Pitcher, W. S., 1965. The stratigraphy and origin of the
 920 Port Askaig boulder bed series (Dalradian). *Geol J* **4**, 343-360.
- 921 Kirschvink, J. L., 1992. Late Proterozoic low-latitude global glaciation: the snow ball
 922 earth. In: Schopf, J. W. a. K., C (Ed.), *The Proterozoic Biosphere*. Cambridge
 923 University Press, Cambridge.
- 924 Knoll, A. H., 2003. The geological consequences of evolution. *Geobiology* **1**, 3-14.
- 925 Knoll, A. H., Javaux, E. J., Hewitt, D., Cohen, P., 2006. Eukaryotic organisms in
 926 Proterozoic oceans. *Philosophical Transactions of the Royal Society B-Biological*
 927 *Sciences* **361**, 1023-1038.
- 928 Levasseur, S., Birck, J., Allègre, C.J., 1999. The osmium riverine flux and oceanic mass
 929 balance of osmium. *Earth and Planetary Science Letters*, **174**, 7-23.

- 930 Li, Z. X., Bogdanova, S. V., Collins, A. S., Davidson, A., De Waele, B., Ernst, R. E.,
 931 Fitzsimons, I. C. W., Fuck, R. A., Gladkochub, D. P., Jacobs, J., Karlstrom, K. E.,
 932 Lu, S., Natapov, L. M., Pease, V., Pisarevsky, S. A., Thrane, K., Vernikovsky, V.,
 933 2008. Assembly, configuration, and break-up history of Rodinia: A synthesis.
 934 *Precambrian Research* **160**, 179-210.
- 935 Li, Z.-X., Evans, D.A.D., 2010. Late Neoproterozoic 40° intraplate rotation within
 936 Australia allows for a tighter-fitting and longer-lasting Rodinia. *Geology*, **39**, 39-
 937 42.
- 938 Litherland, M., 1980. The Stratigraphy of the Dalradian Rocks around Loch Creran,
 939 Argyll. *Scottish Journal of Geology* **16**, 105-123.
- 940 Logan, G. A., Hayes, J. M., Hieshima, G. B., Summons, R. E., 1995. Terminal
 941 Proterozoic reorganization of biogeochemical cycles. *Nature* **376**, 53-56.
- 942 Logan, G. A., Summons, R. E., Hayes, J. M., 1997. An isotopic biogeochemical study of
 943 Neoproterozoic and Early Cambrian sediments from the Centralian Superbasin,
 944 Australia. *Geochimica Et Cosmochimica Acta* **61**, 5391-5409.
- 945 Ludwig, K., 2003. Isoplot/Ex, version 3: a geochronological toolkit for Microsoft Excel.
 946 *Geochronology Center Berkeley*.
- 947 Ludwig, K. R., 1980. Calculation of uncertainties of U-Pb isotope data. *Earth and*
 948 *Planetary Science Letters* **46**, 212-220.
- 949 Macdonald, F.A., Schmitz, M.D., Crowley, J.L., Roots, C.F., Jones, D.S., Maloof, A.C.,
 950 Strauss, J.V., Cohen, P.A., Johnston, D.T., Schrag, D.P., 2010a. Calibrating the
 951 Cryogenian. *Science* **327**, 1241-1243.
- 952 Macdonald, F. A., Cohen, P. A., Dudas, F. O., Schrag, D. P., 2010b. Early
 953 Neoproterozoic scale microfossils in the Lower Tindir Group of Alaska and the
 954 Yukon Territory. *Geology* **38**, 143-146.
- 955 Mao, J., Lehmann, B., Du, A., Zhang, G., Ma, D., Wang, Y., Zeng, M., Kerrich, R., 2002.
 956 Re-Os Dating of Polymetallic Ni-Mo-PGE-Au Mineralization in Lower Cambrian
 957 Black Shales of South China and its geological significance. *Economic Geology*
 958 **97**, 1051-1061.
- 959 Martin, M. W., Grahdankin, D. V., Bowring, S. A., Evans, D. A., D., Fedonkin, M. A.,
 960 Kirschvink, J. L., 2000. Age of Neoproterozoic Bilatarian Body and Trace Fossils,
 961 White Sea, Russia: Implications for Metazoan Evolution. *Science* **288**, 841-845.
- 962 McCay, G. A., Prave, A. R., Alsop, G. I., Fallick, A. E., 2006. Glacial trinity:
 963 Neoproterozoic Earth history within the British-Irish Caledonides. *Geology* **34**,
 964 909-912.
- 965 Meert, J. G., 2007. Testing the Neoproterozoic glacial models. *Gondwana Research* **11**,
 966 573-574.
- 967 Melezhik, V. A., Gorokhov, I. M., Kuznetsov, A. B., Fallick, A. E., 2001.
 968 Chemostratigraphy of Neoproterozoic carbonates: implications for 'blind dating'.
 969 *Terra Nova* **13**, 1-11.
- 970 Melezhik, V. A., Roberts, D., Fallick, A. E., Gorokhov, I. M., 2008. The Shuram-
 971 Wonoka event recorded in a high-grade metamorphic terrane: insight from the
 972 Scandinavian Caledonides. *Geological Magazine* **145**, 161-172.
- 973 Morton, J.P., Long, L.E., 1982. Rb-Sr Ages of Precambrian Sedimentary-Rocks in the
 974 USA. *Precambrian Research*, **18**, (1-2), 133-138.
- 975 Narbonne, G. M., Gehling, J. G., 2003. Life after snowball: The oldest complex
 976 Ediacaran fossils. *Geology* **31**, 27-30.

- 977 Neilson, J. C., Kokelaar, B. P., Crowley, Q. G., 2009. Timing, relations and cause of
 978 plutonic and volcanic activity of the Siluro-Devonian post-collision magmatic
 979 episode in the Grampian Terrane, Scotland. *Journal of the Geological Society*
 980 **166**, 545-561.
- 981 Noble, S. R., Hyslop, E. K., Highton, A. J., 1996. High precision U-Pb monazite
 982 geochronology of the c. 806 Ma Grampian Shear Zone and the implications for
 983 the evolution of the Central Highlands of Scotland. *Journal of the Geological*
 984 *Society*, **153**, 511-514.
- 985 Ogg, J. G., Ogg, G., Gradstein, F.M., 2008. *The Concise Geologic Time Scale*.
 986 Cambridge University Press, Cambridge.
- 987 Ohr, M., Halliday, A.N., Peacor, D.R., 1991 Sr and Nd Isotopic Evidence for Punctuated
 988 Clay Diagenesis, Texas Gulf-Coast. *Earth and Planetary Science Letters*, **105**,
 989 110-126.
- 990 Oliver, G. J. H., 2001. Reconstruction of the Grampian episode in Scotland: its place in
 991 the Caledonian Orogeny. *Tectonophysics* **332**, 23-49.
- 992 Pattison, D. R. M., 2006. The fate of graphite in prograde metamorphism of pelites: An
 993 example from the Ballachulish aureole, Scotland. *Lithos* **88**, 85-99.
- 994 Pattison, D. R. M., Harte, B., 1997. The geology and evolution of the Ballachulish
 995 Igneous Complex and Aureole. *Scot J Geol* **33**, 1-29.
- 996 Peucker-Ehrenbrink, B., Jahn, B.-m., 2001. Rhenium-osmium isotope systematics and
 997 platinum group element concentrations: Loess and the upper continental crust.
 998 *Geochem. Geophys. Geosyst.* **2**.
- 999 Piasecki, M. A. J., 1980. New light on the Moine rocks of the Central Highlands of
 1000 Scotland. *Journal of the Geological Society* **137**, 41-59.
- 1001 Prave, A. R., 1999. The Neoproterozoic Dalradian Supergroup of Scotland: an alternative
 1002 hypothesis. *Geological Magazine* **136**, 609-617.
- 1003 Prave, A. R., Fallick, A. E., Thomas, C. W., Graham, C. M., 2009a. A composite C-
 1004 isotope profile for the Neoproterozoic Dalradian Supergroup of Scotland and
 1005 Ireland. *Journal of the Geological Society* **166**, 845-857.
- 1006 Prave, A. R., Strachan, R. A., Fallick, A. E., 2009b. Global C cycle perturbations
 1007 recorded in marbles: a record of Neoproterozoic Earth history within the
 1008 Dalradian succession of the Shetland Islands, Scotland. *Journal of the Geological*
 1009 *Society* **166**, 129-135.
- 1010 Preiss, W. V., 2000. The Adelaide Geosyncline of South Australia and its significance in
 1011 Neoproterozoic continental reconstruction. *Precambrian Research* **100**, 21-63.
- 1012 Pringle, J., 1939. The discovery of Cambrian trilobites in the Highland Border rocks near
 1013 Callander, Perthshire. *Report of the British Association for the Advancement of*
 1014 *Science* **252**.
- 1015 Rainbird, R.H., Hamilton, M.A., Young, G.M., 2001. Detrital zircon geochronology and
 1016 provenance of the Torridonian, NW, Scotland: *Journal of the Geological Society*,
 1017 **158**, 15-27
- 1018 Ravizza, G., Turekian, K. K., 1989. Application of the ^{187}Re - ^{187}Os system to black shale
 1019 geochronometry. *Geochimica et Cosmochimica Acta* **53**, 3257-3262.
- 1020 Ravizza, G., Turekian, K.K., Hay, B.J., 1991. The geochemistry of rhenium and osmium
 1021 in recent sediments from the Black Sea. *Geochim. Cosmochim. Acta.* **55**, 3741-
 1022 3752.

- 1023 Rogers, G., Dunning, G. R., 1991. Geochronology of appinitic and related granitic
1024 magmatism in the W Highlands of Scotland: constraints on the timing of
1025 transcurrent fault movement. *Journal of the Geological Society* **148**, 17-27.
- 1026 Rooney, A. D., Selby, D., Houzay, J.-P., Renne, P. R., 2010. Re-Os geochronology of a
1027 Mesoproterozoic sedimentary succession, Taoudeni basin, Mauritania:
1028 Implications for basin-wide correlations and Re-Os organic-rich sediments
1029 systematics. *Earth and Planetary Science Letters* **289**, 486-496.
- 1030 Sawaki, Y., Kawai, T., Shibuya, T., Tahata, M., Omori, S., Komiya, T., Yoshida, N.,
1031 Hirata, T., Ohno, T., Windley, B. F., Maruyama, S., 2010. $^{87}\text{Sr}/^{86}\text{Sr}$
1032 chemostratigraphy of Neoproterozoic Dalradian carbonates below the Port Askaig
1033 Glaciogenic Formation, Scotland. *Precambrian Research* **179**, 150-164.
- 1034 Scott, C., Lyons, T.W., Bekker, A., Shen, Y., Poulton, S.W., Chu, X., Anbar, A.D., 2008.
1035 Tracing the stepwise oxygenation of the Proterozoic ocean. *Nature*, **452**, 456-460.
- 1036 Selby, D., 2007. Direct Rhenium-Osmium age of the Oxfordian-Kimmeridgian boundary,
1037 Staffin bay, Isle of Skye, U.K., and the Late Jurassic time scale. *Norwegian*
1038 *Journal of Geology*. **87**, 9.
- 1039 Selby, D., 2009. U-Pb zircon geochronology of the Aptian / Albian boundary implies that
1040 the GL-O international glauconite standard is anomalously young. *Cretaceous*
1041 *Research*, **30**, 1263-1267.
- 1042 Selby, D., Creaser, R. A., 2003. Re-Os geochronology of organic rich sediments: an
1043 evaluation of organic matter analysis methods. *Chemical Geology* **200**, 225-240.
- 1044 Selby, D., Creaser, R. A., 2005. Direct radiometric dating of the Devonian-Mississippian
1045 time-scale boundary using the Re-Os black shale geochronometer. *Geology* **33**,
1046 545-548.
- 1047 Selby, D., Creaser, R. A., Stein, H. J., Markey, R. J., Hannah, J. L., 2007. Assessment of
1048 the Re^{-187} decay constant by cross calibration of Re-Os molybdenite and U-Pb
1049 zircon chronometers in magmatic ore systems. *Geochimica Et Cosmochimica*
1050 *Acta* **71**, 1999-2013.
- 1051 Selby, D., Mutterlose, J., Condon, D.J., 2009. U-Pb and Re-Os geochronology of the
1052 Aptian / Albian and Cenomanian / Turonian stage boundaries and Re-Os
1053 systematics in organic-rich sediments. *Chemical Geology*, **265**, 394-409.
- 1054 Slack, J.F., Jiang, W.T., Peacor, D.R., Okita, P.M., 1992. Hydrothermal and metamorphic
1055 berthierine from the Kidd Creek Volcanogenic Massive Sulfide Deposit,
1056 Timmins, Ontario. *Canadian Mineralogist*. **30**, 1127-1142.
- 1057 Smith, M., Robertson, S., Rollin, K. E., 1999. Rift basin architecture and stratigraphical
1058 implications for basement-cover relationships in the Neoproterozoic Grampian
1059 Group of the Scottish Caledonides. *Journal of the Geological Society* **156**, 1163-
1060 1173.
- 1061 Smoliar, M. I., Walker, R. J., Morgan, J. W., 1996. Re-Os isotope constraints on the age
1062 of Group IIA, IIIA, IVA, and IVB iron meteorites. *Science* **271**, 1099-1102.
- 1063 Soper, N. J., 1994. Was Scotland a Vendian RRR junction? *Journal of the Geological*
1064 *Society* **151**, 579-582.
- 1065 Soper, N. J., England, R. W., 1995. Vendian and Riphean rifting in NW Scotland.
1066 *Journal of the Geological Society* **152**, 11-14.
- 1067 Soper, N. J., Ryan, P. D., Dewey, J. F., 1999. Age of the Grampian orogeny in Scotland
1068 and Ireland. *Journal of the Geological Society* **156**, 1231-1236.
- 1069 Spencer, A. M., 1971. Late Precambrian glaciation in Scotland. *Memoirs of the*
1070 *Geological Society of London* **6**, 1-100.

- 1071 Strachan, R. A., Smith, M., Harris, A.L., Fettes, D.J., 2002. The Northern Highland and
 1072 Grampian terranes. In: Trewin, N. H. (Ed.), *The Geology of Scotland*. The
 1073 Geological Society, London.
- 1074 Sun, W., Arculus, R. J., Bennett, V. C., Eggins, S. M., Binns, R. A., 2003. Evidence for
 1075 rhenium enrichment in the mantle wedge from submarine arc-like volcanic
 1076 glasses (Papua New Guinea). *Geology* **31**, 845-848.
- 1077 Tanner, P. W. G., Alsop, G. I., Hutton, D. H. W., 2005. Discussion on evidence for a
 1078 major Neoproterozoic orogenic unconformity within the Dalradian Supergroup of
 1079 NW Ireland. *Journal of the Geological Society* **162**, 221-224.
- 1080 Tanner, P. W. G., Evans, J. A., 2003. Late Precambrian U-Pb titanite age for peak
 1081 regional metamorphism and deformation (Knoydartian orogeny) in the western
 1082 Moine, Scotland. *Journal of the Geological Society* **160**, 555-564.
- 1083 Tanner, P. W. G., Pringle, M. S., 1999. Testing for the presence of a terrane boundary
 1084 within Neoproterozoic (Dalradian) to Cambrian siliceous turbidites at Callander,
 1085 Perthshire, Scotland. *Journal of the Geological Society* **156**, 1205-1216.
- 1086 Tanner, P. W. G., Sutherland, S., 2007. The Highland Border Complex, Scotland: a
 1087 paradox resolved. *Journal of the Geological Society* **164**, 111-116.
- 1088 Thomas, C., Graham, C., Ellam, R., Fallick, A., 2004. $^{87}\text{Sr}/^{86}\text{Sr}$ chemostratigraphy of
 1089 Neoproterozoic Dalradian limestones of Scotland and Ireland: constraints on
 1090 depositional ages and time scales. *Journal of the Geological Society* **161**, 229-
 1091 242.
- 1092 Thomson, J., 1871. On the occurrence of pebbles and boulders of granite in schistose
 1093 rocks on Islay, Scotland *Report of the 40th Meeting of the British Association for*
 1094 *the Advancement of Science*, Liverpool.
- 1095 Thomson, J., 1877. On the geology of the island of Islay. *Transactions of the Geological*
 1096 *Society of Glasgow* **5**, 200-222.
- 1097 Tilley, C. E., 1925. A preliminary survey of metamorphic zones in the southern
 1098 Highlands of Scotland. *Quarterly Journal of the Geological Society of London* **81**.
- 1099 Trindade, R. I. F., Macouin, M., 2007. Palaeolatitude of glacial deposits and
 1100 palaeogeography of Neoproterozoic ice ages. *Comptes Rendus Geosciences* **339**,
 1101 200-211.
- 1102 Vidal, G., Moczydlowska-Vidal, M., 1997. Biodiversity, Speciation, and Extinction
 1103 Trends of Proterozoic and Cambrian Phytoplankton. *Paleobiology* **23**, 230-246.
- 1104 Voll, G., Topel, J., Pattison, D.R.M., Seifert, F., 1991. Equilibrium and Kinetics in
 1105 Contact Metamorphism: The Ballachulish Igneous Complex and its Aureole. .
 1106 Springer Verlag, Heidelberg.
- 1107 Walker, R. J., Horan, M. F., Morgan, J. W., Becker, H., Grossman, J. N., Rubin, A. E.,
 1108 2002a. Comparative ^{187}Re - ^{187}Os systematics of chondrites: Implications regarding
 1109 early solar system processes. *Geochimica Et Cosmochimica Acta* **66**, 4187-4201.
- 1110 Walker, R. J., Prichard, H. M., Ishiwatari, A., Pimentel, M., 2002b. The osmium isotopic
 1111 composition of convecting upper mantle deduced from ophiolite chromites.
 1112 *Geochimica Et Cosmochimica Acta* **66**, 329-345.
- 1113 Walsh, J. A., 2007. The use of the scanning electron microscope in the determination of
 1114 the mineral composition of Ballachulish slate. *Materials Characterization* **58**,
 1115 1095-1103.
- 1116 Yang, G., Hannah, J. L., Zimmerman, A., Stein, H. J., Bekker, A., 2009. Re-Os
 1117 depositional age for Archean carbonaceous slates from the southwestern Superior

1118 Province: Challenges and insights. *Earth and Planetary Science Letters* **280**, 83-
1119 92.

1120 Zhou, C., Tucker, R., Xiao, S., Peng, Z., Yuan, X., Chen, Z., 2004. New constraints on
1121 the ages of Neoproterozoic glaciations in south China. *Geology* **32**, 437-440.

1122

1123

1124 **Figure Captions**

1125 Figure 1: Simplified geological and location map highlighting the fourfold division of the
1126 Dalradian Supergroup of the Grampian Terrane (modified from Harris et al., 1994;
1127 Thomas et al., 2004). Abbreviations of sampling locations: BA – Ballachulish Slate
1128 quarry; LQ - Leny Limestone quarry.

1129

1130 Figure 2: Generalised stratigraphic column of the Dalradian Supergroup with glaciogenic
1131 horizons and the purported Bitter Springs anomaly suggested by Prave et al., (2009) but
1132 refuted by the new Re-Os geochronology data. See text for details. BA – Ballachulish
1133 Slate Formation; LQ – Leny Limestone Formation. (1. Halliday et al., 1989; 2. Dempster
1134 et al., 2002; 3. This study; 4. Noble et al., 1996). Modified from Prave et al. (2009a).

1135

1136 Figure 3: Re-Os isochron diagram for the Ballachulish Slate Formation using various
1137 digestion mediums a) the $\text{CrO}_3\text{-H}_2\text{SO}_4$ digestion method, b) inverse *aqua-regia* digestion,
1138 c) both digestion analyses ($\text{CrO}_3\text{-H}_2\text{SO}_4$ solid line, inverse *aqua-regia* dashed line). Inset
1139 diagrams show the deviation of each point from the $\text{CrO}_3\text{-H}_2\text{SO}_4$ best-fit regression. A
1140 Model 1 isochron is accomplished by assuming scatter along the regression line is
1141 derived only from the input 2σ uncertainties for $^{187}\text{Re}/^{188}\text{Os}$ and $^{187}\text{Os}/^{188}\text{Os}$, and ρ (rho).

1142

1143 Figure 4: Re-Os isochron diagram for the Leny Slate Member. The dashed line represents
1144 a 512 Ma reference line with the Os_i value of 0.8 representing Cambrian seawater (Mao
1145 et al., 2002; Jiang et al., 2003). The 512 Ma age assigned for the Leny Limestone is based
1146 on a trilobite fauna (Fletcher and Rushton, 2007). See text for discussion.

1147

1148 Figure 5: Graphic illustration of Re-Os geochronology data and Os_i values for
1149 Cryogenian and Sturtian (*sensu stricto*) pre and post glacial horizons. See text for
1150 discussion. Data from 1 = Ballachulish Slate Formation (this study); 2 = Aralka

1151 Formation (Kendall et al., 2006); 3 = Tapley Hill Formation (Kendall et al., 2006); 4 =
1152 Black River Dolomite (Kendall et al., 2009a)

1153

1154 **Tables**

1155 Table 1: Re-Os isotope data for the Ballachulish Slate and Leny Slate samples.

Accepted Manuscript

Table 1

Re-Os isotope data for the Ballachulish Slate and Leny Limestone Formations

Sample ^a	Re (ppb)	±	Os (ppt)	±	¹⁹² Os (ppt)	±	¹⁸⁷ Re/ ¹⁸⁸ Os	±	¹⁸⁷ Os/ ¹⁸⁸ Os	±	rho ^b	Os _i ^c
<i>Ballachulish Slate samples</i>												
Balla 2B	1.20	0.01	46.0	0.5	13.9	0.2	172.6	2.3	2.944	0.044	0.731	1.04
Balla 2B ar	1.08	0.00*	43.8	0.4	13.3	0.2	161.3	1.9	2.876	0.042	0.763	1.09
Balla 2C	1.85	0.01	52.2	0.5	14.5	0.2	253.8	3.2	3.841	0.055	0.758	1.04
Balla 2C ar	1.77	0.01	53.5	0.5	15.3	0.2	230.8	2.6	3.564	0.050	0.745	1.01
Balla 3	1.69	0.01	40.9	0.5	10.8	0.2	311.7	4.6	4.478	0.072	0.813	1.04
Balla 3 ar	1.68	0.01	40.9	0.5	10.9	0.1	308.2	4.1	4.364	0.067	0.805	0.96
Balla 5B	0.29	0.01	29.2	0.3	10.1	0.2	56.5	1.4	1.660	0.029	0.482	1.04
Balla 5B ar	0.30	0.00*	30.6	0.3	10.6	0.1	55.6	0.8	1.593	0.026	0.767	0.98
Balla 6	0.39	0.02	25.5	0.7	8.4	0.5	93.3	6.4	2.060	0.142	0.645	1.03
Balla 6 ar	0.30	0.01	41.4	0.6	16.7	0.6	41.4	1.3	1.472	0.050	0.511	1.01
<i>Leny Slate Samples</i>												
L1	55.8	0.2	487.7	3.1	107.1	0.5	1036.8	5.6	6.874	0.033	0.716	-1.97
L2	55.4	0.2	431.0	3.0	89.8	0.4	1228.0	7.2	7.649	0.041	0.756	-2.83
L3	49.4	0.2	430.6	3.0	92.2	0.5	1065.8	6.2	7.239	0.038	0.759	-1.85
L4	50.9	0.2	419.2	3.0	85.0	0.4	1192.4	7.2	8.075	0.045	0.778	-2.10
L5	49.6	0.2	424.1	3.0	88.4	0.5	1117.0	6.7	7.642	0.042	0.771	-1.89
L6	51.2	0.2	443.0	3.0	92.1	0.4	1107.2	6.3	7.691	0.039	0.755	-1.76
L7	66.1	0.2	633.1	4.1	146.3	0.6	898.4	4.5	6.162	0.031	0.583	-1.50
L8	46.2	0.2	447.0	3.2	99.7	0.5	921.5	5.4	6.650	0.040	0.682	-1.21
L9	57.7	0.2	515.9	3.3	114.5	0.5	1001.9	5.2	6.716	0.031	0.680	-1.83

^a "ar" denotes inverse aqua regia digestion^{*} Uncertainty is less than 0.01^b Rho is the associated error correlation (Ludwig, 1980).^c Os_i = initial ¹⁸⁷Os/¹⁸⁸Os isotope ratio calculated at 659 Ma for the Ballachulish Slate samples and at 512 Ma for the Leny Slate samples

